Durham E-Theses

Regulation of cell fate by the IRE1 α-TRAF2-JNK axis

YOUNG, CHRISTOPHER,MATTHEW,THOMA

How to cite:

YOUNG, CHRISTOPHER,MATTHEW,THOMA (2018) *Regulation of cell fate by the IRE1 α-TRAF2-JNK axis*, Durham theses, Durham University. Available at Durham E-Theses Online: http://etheses.dur.ac.uk/12911/

Use policy

The full-text may be used and/or reproduced, and given to third parties in any format or medium, without prior permission or charge, for personal research or study, educational, or not-for-profit purposes provided that:

- a full bibliographic reference is made to the original source
- a link is made to the metadata record in Durham E-Theses
- the full-text is not changed in any way

The full-text must not be sold in any format or medium without the formal permission of the copyright holders.

Please consult the full Durham E-Theses policy for further details.

Academic Support Office, Durham University, University Office, Old Elvet, Durham DH1 3HP
e-mail: e-theses.admin@dur.ac.uk Tel: +44 0191 334 6107
http://etheses.dur.ac.uk

Durham University

Regulation of cell fate by the IRE1 α-TRAF2-JNK axis

Characterisation of IRE1 α kinase domain

Christopher Matthew Thomas Young

This thesis is submitted as part of the requirements for the award of
Master of Science by Research
Biological Sciences

Department of Biosciences
Durham University
2018

Abstract

Eukaryotic cells produce proteins continuously through translation, folding and quality control within the endoplasmic reticulum (ER). When unfolded proteins accumulate in the endoplasmic reticulum the unfolded protein response (UPR) attempts to restore cellular function by reducing the load of unfolded proteins. If cellular function is not restored the unfolded protein response causes cell death through apoptosis. The only known unfolded protein response protein in lower eukaryotes is inositol-requiring enzyme 1 α (IRE1 α). In this thesis we investigated whether the kinase domain of inositol-requiring enzyme 1 α alone regulates apoptosis or whether the RNase domain is required for apoptotic cell death through the unfolded. We found evidence to suggest that inositol-requiring enzyme 1 α kinase domain alone does not cause apoptosis. Juxtaposing these results, the kinase domain alone causes the presence of phosphorylated proteins that are precursors to apoptosis. Two theories are that mutations made to deactivate the RNase domain effected the folding of the kinase domain reducing its potency. The second theory is that inositol-requiring enzyme 1 α RNase domain plays an unknown role in apoptotic cell death in the unfolded protein response.

Contents

List of Abbreviations

Abbreviation	Explanation
˚C	Celsius
µg	Microgram
µl	Microliter
Aa	Amino acids
ADP	Adenosine diphosphate
AP20187	B-B homodimer
ASK1	Apoptosis signal-regulating kinase 1
ASL	Anticodon stem-loop
ATF6	Activating transcription factor 6
ATP	Adenosine triphosphate
Bip	Binding immunoglobulin protein
bp	Base pairs
cDNA	complementary deoxyribonucleic acid
d	Days
DEPC H_2O	Diethyl pyrocarbonate treated water
dH_2O	Double distilled water
DMEM	Dulbecco's modified eagle media
ER	Endoplasmic reticulum
ERAD	Endoplasmic reticulum associated degradation
ERN1	Endoplasmic reticulum to nucleus signalling 1
FBS	Fetal bovine serum
g	Gravitational force
h	Hour
HEK	Human embryonic kidney
INS-1	Insulin secreting beta cell line - 1
IRE1 α	Inositol-requiring enzyme 1 α
IRE1 β	Inositol-requiring enzyme 1 β
JNK	c-Jun N-terminal kinase
kDa	Kilo-Dalton
LB	Lysogeny broth
M	Molar
MAPK	Mammalian mitogen-activated protein kinase
MAPKKK / MAPK4	Mammalian mitogen-activated protein kinase kinase kinase
mg	Milligram
min	Minute
ml	Millilitre
mM	Micro molar
mRNA	Messenger ribonucleic acid
MTT	3-[4,5-Dimethylthiazol-2-yl]-2,5-diphenyltetrazolium bromide; Thiazolyl blue

nm	Nano meters
nM	Nano molar
OPRA	Optimal protein RNA area algorithm
oz	Ounce
PARP-1	Poly ADP-ribose polymerase 1
PCR	Polymerase chain reaction
PERK	Protein kinase R (PKR)-like endoplasmic reticulum kinase
phe	Phenylalanine
P-IRE1 α	Phosphorylated inositol-requiring enzyme 1 α
P-JNK	Phosphorylated c-Jun N-terminal kinase
RIDD	Regulated IRE1-dependent decay of mRNA
RNA	ribonucleic acid
RNase	Ribonuclease
rpm	Revolutions per minute
RT	Room temperature
s	Second
SAPKs	stress-activated protein kinases
sds	Sodium dodecyl sulfate
SOC	Super optimal broth
TBST	Tris-buffered saline + Tween
tetR	Tet repressor proteins
TNF	Tumor necrosis factor
TRAF2	TNF receptor-associated factor 2
tRNA	Transfer ribonucleic acid
UPR	Unfolded protein response
UV	Ultraviolet
V	Volts
v/v	Volume to volume
w/v	Weight to volume
WT	Wild type
XBP1	X-box binding protein 1
XBP1s	Spliced X-box binding protein 1

1. Introduction

1.1 ER stress

Cells have mechanisms to respond to any perturbation and maintain homeostasis, the maintenance of the endoplasmic reticulum (ER) is an important function of all cells. The ability to respond to perturbations of the ER, 'ER stress', is necessary for cell survival; if unresolved or under chronic activation will lead to the activation of a signalling network culminating in cell death (Ozcan and Tabas, 2012). ER stress has multiple causes. It can be caused by increased protein synthesis or misfolding rates exceeding the capacity of chaperones 'client load' (Ron and Walter, 2007). ER stress can artificially be triggered by alteration of calcium stores in the ER lumen or disturbance of the redox balance (Ron and Walter, 2007).

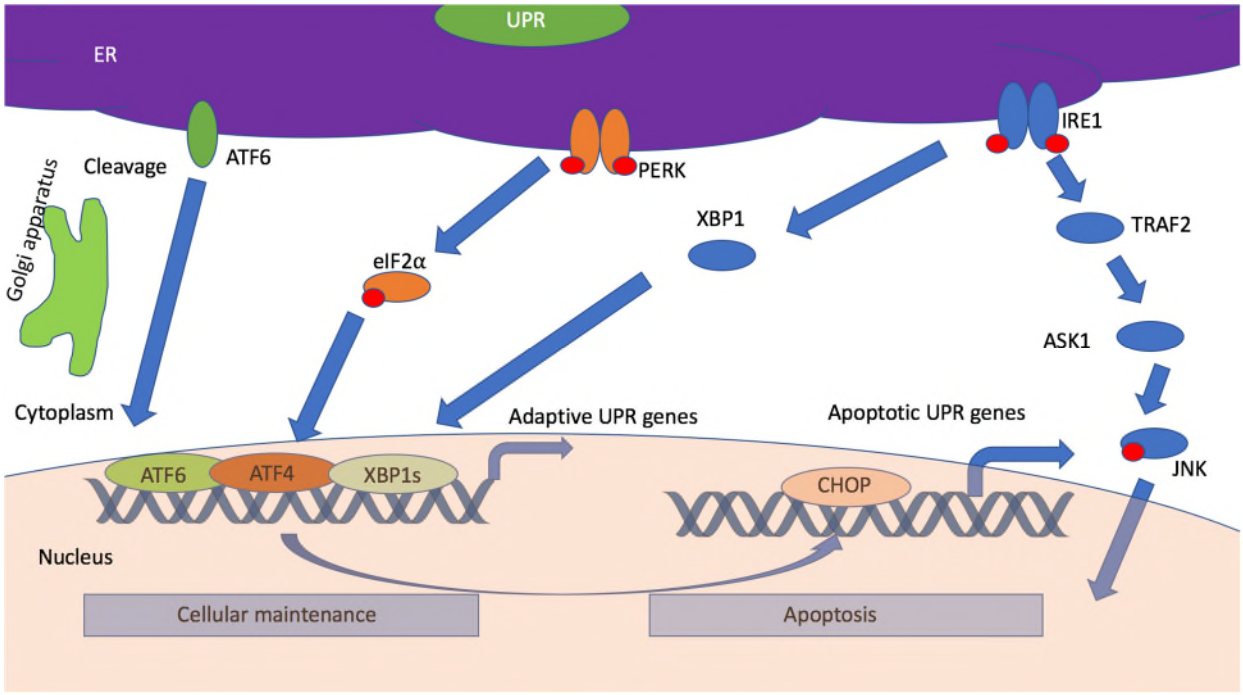

Figure 1.1.1, Overview of ER stress signalling in eukaryotes via the ER transmembrane proteins ATF6, PERK and IRE1 α (Kadowaki and Nishitoh, 2013).

ER stress is sensed by three upstream signalling proteins in multicellular eukaryotes that activate a cascade of corrective actions; combined this is known as the unfolded protein response (UPR) as shown in Figure 1.1.1, (Tabas and Ron, 2011). The oldest ER stress recognition pathway receptor protein is a combined nuclease and kinase called inositol-requiring 1 IRE1 α. IRE1 α is expressed as two isoforms IRE1 α, systemic, and IRE1 β, which is restricted to the gastrointestinal and respiratory tracts (Tabas and Ron, 2011). ER-stress transducers such as IRE1 α, become activated when there is an imbalance of unfolded proteins and chaperones (Tabas and Ron, 2011). The mechanism for detection of ER stress is likely initiated by changes in heterologous protein interactions such as dissociation of chaperones such as BiP oligomerization in ER-stressed cells (Ron and Walter, 2007).

1.2 The unfolded protein response

The endoplasmic reticulum (ER) is an organelle that contains chaperones and enzymes to promote the folding of secretory proteins (Han et al., 2009). A delicate balance exists between translation and folding capacity; when translation outpaces folding capacity unfolded proteins accumulate and result in ER stress (Han et al., 2009). ER stress is detected by three proteins in mammalian cells, IRE1 α, PERK and ATF6, that signal intracellular signalling pathways called the unfolded protein response (UPR) (Han et al., 2009). The UPR sensors upregulate transcription of genes encoding ER chaperones, oxidoreductases and ER-associated degradation (ERAD) components (Travers et al., 2000) and phospholipid biosynthetic genes (Travers et al., 2000). The UPR exerts a translational block during ER stress as a form of adaptive homoeostasis by reducing ER protein load (Harding et al., 2001). The UPR upregulates folding capacity and degrades unfolded proteins (Ron and Walter, 2007). If ER stress reduces, negative feedback leads to waning of the UPR signal and recovery of the cell (Merksamer et al., 2008). Alternatively, if misfolded protein stress is too great cells are removed through UPR-mediated apoptosis; when large numbers of cells die in vital organs this leads to pathological disease (Kaufman, 2002). The mechanism for cell fate to choose adaption versus apoptosis through the UPR is unclear due to heavy crosstalk. The UPR apoptosis/adaption is likely controlled by the three unfolded protein sensors (Han et al., 2009).

1.3 Structure of IRE1 α

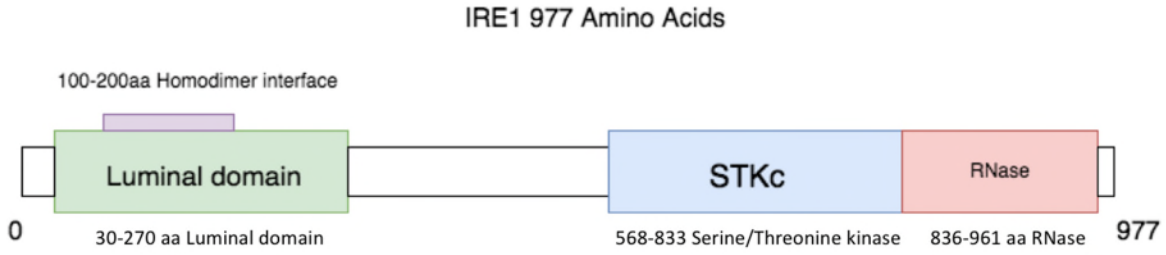

Figure 1.3.1, Diagram of IRE1 α domain organisation. Domain information from NCBI protein blast AAI30408.1 Luminal domain 30-270 aa, (STKc) Serine/Threonine kinase 568-833 aa, (RNase) Ribonuclease 836-961 aa.

The gene *ERN1* encodes the type 1 transmembrane ER to nucleus signalling 1 protein also known as serine/threonine-protein kinase/endoribonuclease Inositol-requiring 1 (IRE1) (Tirasophon, Welihinda and Kaufman, 1998). As shown in Figure 1.3.1, the luminal domain of IRE1 α 30-270 amino acids localises within the ER membrane and contains the homodimer interface that initiates the formation of oligomers in the presence of unfolded proteins in the ER (Aragon et al., 2009; Credle et al., 2005; Zhou et al., 2006). The serine/threonine kinase resides at residues 568-833. This domain catalyses the transfer of the gamma-phosphoryl group from ATP to serine and threonine residues of target proteins including other IRE1 α. The ribonuclease domain resides between residues 835-961 and cleaves the exon-intron junctions in the mRNA for the transcription factor controlled by IRE1 α and catalyses the degradation of RNA reducing the folding demand on chaperones. IRE1 α is expressed in all cells and tissues in metazoans and is the only component of the UPR in yeast genomes found in eukaryotes (Tirasophon, Welihinda and Kaufman, 1998). Given that this protein is conserved from yeast while other UPR proteins are only occur in metazoans, it is likely to have a major role in the UPR.

1.4 mRNA degradation

During ER stress the UPR uses signalling to regulate ER protein folding capacity as well as degrading ER localised mRNA to maintain homoeostasis (Han et al., 2009). ER stress in yeast induces oligomerisation and autophosphorylation of IRE1 α luminal domains resulting in the assembly of the cytosolic kinase and RNase into a defined three-dimensional structure. The oligomer is stabilised by phosphates from autophosphorylation of the kinase domain allowing juxtaposition of the RNase domains presumably activating them in yeast (Korennykh et al., 2011).

IRE1 α autophosphorylation also leads to endonucleolytic decay of ER-localised mRNAs including those that encode chaperones, via the RNase domain (Han et al., 2009). The endoribonuclease (RNase) domain also initiates non-conventional mRNA splicing (Korennykh et al., 2011). This splicing leads to production of a transcription factor that controls UPR target genes (Korennykh et al., 2011), X-box binding protein 1 (XBP1) mRNA splicing results in the active transcription factor XBP1s (Calfon et al., 2002; Yoshida et al., 2001).

IRE1 α uses amino acid side chains for catalysis of the RNase activity (Dong et al., 2001). IRE1 α uses histidine 1061 and tyrosine 1043 residues as general acid-general base pair for transition state stabilisation, coordination of the scissile phosphate occurs through asparagine 1057 and arginine 1056 (Tirasophon, 2000; Korennykh et al., 2011). IRE1 α can specifically cleave anticodon stem-loop (ASL) or tRNA phe and HAC1 XBP1 (Korennykh et al., 2011). It has been suggested that from the crystal structure of the RNase dimer each contain two independent catalytic centres in each monomer simultaneously accommodating the two RNA stem-loops (Tirasophon, 2000). While each RNase monomer contains separate catalytic apparatus for RNA cleavage, it is presumed that two RNase subunits are required to contribute to RNA stem-loop docking (Korennykh et al., 2011). Given the conservation of key residues in known homologues between yeast and higher eukaryotic IRE1 the process for mRNA degradation is likely to have been conserved as well (Korennykh et al., 2011).

1.5 *XBP1* mRNA splicing

Non-conventional splicing of *HAC1* mRNA is seen in yeast and XBP1 mRNA in metazoans by cleavage of exons via two conserved sites (Dong et al., 2001), (Lee et al., 2008), (Korennykh et al., 2011). IRE1 α recognises conserved sites in XBP1 characterised by a stem containing five Watson-Crick base pairs and a seven-residue loop with a consensus sequence CNGNNGN (Gonzalez, EMBO J. 1999). The exons are re-joined by tRNA ligase in yeast and in metazoans leading to the formation of the active transcription factor XBP1s (Dong et al., 2001; Lee et al., 2008; Korennykh et al., 2011; Cox et al. 1993, 1996; Sidrauski et al., 1996, 1997; Calfon et al., 2001; Shen et al., 2001; Yoshida et al., 2001; Lee at l., 2002). Analysis by optimal protein RNA area algorithm (OPRA) suggestes interaction between the binding of IRE1 α and XBP1 mRNA (Korennykh et al., 2011). OPRA suggests that there is a single RNA binding site at the centre of the RNase dimer that interacts with XBP1 mRNA with the rest of the surface predicted to be unlikely to interact with RNA (Tirasophon, 2000). The binding site properties are likely due to electron density at the core. This is formed of eight residues

located proximal to the substrate binding site contribute to the acid base catalysis leading to the formation of the 2', 3'-cyclic phosphate bond (Korennykh et al., 2011). IRE1 α therefore has two functions *in vivo* requiring RNase domain, initiating XBP1 mRNA splicing through site-specific cleavage and ER-localised mRNA decay.

1.6 Kinase activity

The use of kinase inhibitors has been shown to activate RNase function, bypassing autophosphorylation through an alternative route that results in XBP1 splicing but does not promote mRNA decay or apoptosis (Han et al., 2009). It is believed that cell fate between apoptosis or survival is dependent on either kinase or RNase activity (Han et al., 2009). Evidence suggests initial kinase activation translates to downstream effects that restore homeostasis and promote survival. Persistent activation of IRE1 α kinase domain signal inability to adapt to stress and trigger cell fate switch to apoptosis (Han et al., 2009). Under this hypothesis an active kinase/RNase-dead IRE1 α mutant should retain the cytotoxic ability of WT (Wild Type) IRE1 α, perhaps more so due to the lack of XBP1s effects. As IRE1 α has both apoptotic and survival components, loss of the RNase domain should remove the survival processes resulting in increased chances of apoptosis. Han et al., 2009 produced mutants with key mutations in the RNase domain, K907A and N906A. These mutants should have exhibited active kinase/RNase-dead, although these mutants did not induce apoptosis. It is therefore suggested that apoptotic signals from WT IRE1 α require active RNase as well as kinase to induce apoptosis (Han et al., 2009). Paradoxically the results of Han et al., 2009 have also suggested that RNase activity of IRE1 α leads to effectors of both survival and apoptosis outputs.

Although mutants K907A and N906A suggest active kinase/RNase-dead IRE1 α is unable to induce apoptosis, given that the RNase and kinase domains are adjacent, mutation may alter three dimensional structure and function of IRE1 α. Continuing to produce mutations in key RNase residues might produce an active kinase/RNase-dead IRE1 α mutant with the wild type three dimensional structure.

1.7 JNK activation via ASK1

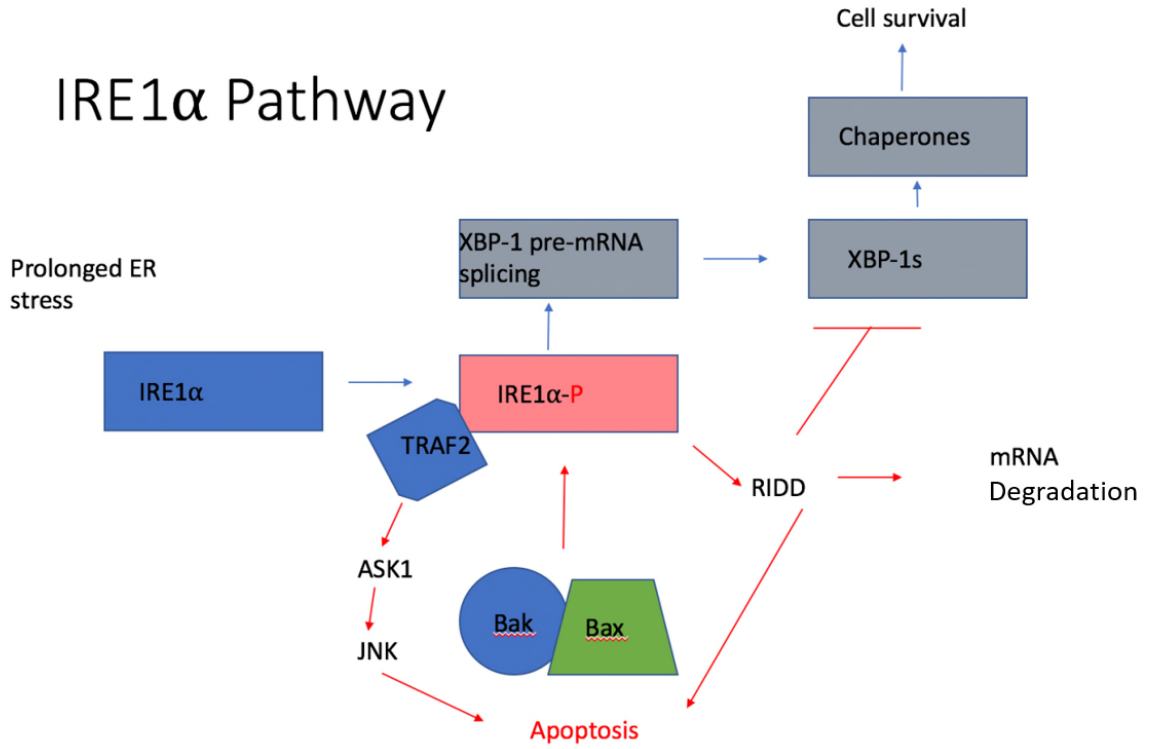

Figure 1.7.1, Overview of IRE1 α intracellular stress signalling pathway caused by prolonged ER stress (Kadowaki and Nishitoh, 2013). This diagram shows the two outcomes caused by IRE1 α activation, cell survival or apoptosis. P-IRE1 α cleaves XBP-1 pre-mRNA resulting in the active XBP-1s a transcription factor that interacts with chaperones to regulate gene expression resulting in reduced ER stress and cell survival. If ER stress is maintained apoptosis is caused by activation of the TRAF2 pathway though ASK1 and JNK.

In diseases such as Huntington, spinocerebellar ataxias and diabetes mellitus the accumulation of polyQ fragments from mutant genes forms aggregates in the cytoplasm/nucleus causing a toxic effect that leads to cell death (Kakizuka 1998; Paulson et al. 2000). PolyQ induces ER stress leading to IRE1 α dimerization, ER stress also was shown to induce TRAF2–ASK1 complex formation that leads to downstream signalling that activates JNK as shown in Figure 1.7.1, (Nishitoh, 2002). ASK1 therefore plays a role mediating proteasome dysfunction and ER stress-induced neuronal cell death, an important role in the neuropathological alterations occurring in polyQ diseases (Nishitoh, 2002). ASK1 plays essential roles in stress-induced apoptosis, ASK1 deficient mice show suppressed TNF and H_2O_2 induced apoptosis (Tobiume et al. 2001), with neurons derived from *ASK1*$^{-/-}$ mice showing resistance to ER stress (Nishitoh, 2002). ASK1 has been shown to only associate with IRE1 α in the presence of TRAF2, although this evidence was obtained through overexpression and has not be confirmed *in vivo*. It is possible that ER stress induces the formation of IRE1 α -TRAF2-ASK1 complex on the ER outer membrane leading to the downstream ASK1-JNK pathway through TNF oxidative stress-induced JNK activation and apoptosis (Ichijo et al. 1997; Saitoh et al. 1998; Tobiume et al. 2001). Apoptosis signal-regulating kinase ASK1 has shown experimental evidence to suggest that it directly interacts with TNF receptor-associated factor 2 TRAF2 (Nishitoh et al. 1998). JNK is activated by mammalian mitogen-activated protein kinase (MAPK) kinase kinase (MAPKKK) the research community assume that active IRE1 α triggers a TNF signaling pathway TRAF2–ASK1–SEK1/MKK4–JNK cascade (Nishitoh et al. 1998). Although JNK activation is linked to IRE1 α -TRAF2-ASK1, ASK1 negative cell lines still have residual JNK activation by TRAF2 therefore

there may be a redundant pathway involving GCK/GCKR– MEKK1 (Yuasa et al. 1998). Consistently, TNF-induced JNK activation was partially, but not completely, lost in *ASK1*−/− mutants this shows that JNK activation can be activated via redundant pathway but ER stress induced activation is highly specific to ASK1 pathway (Nishitoh, 2002). Therefore JNK activation can be caused without the ASK1 pathway, although the ER stress activation and apoptosis of interest is specific to IRE1 α pathway.

The results of (Urano, 2000) suggest that ER stress induced IRE1 α kinase activation is important in the recruitment of TRAF2 while endonuclease activity is dispensable. ER stress through a cascade leads to the activation of c-jun amino-terminal kinases, IRE1 α -/- fibroblasts had impaired JNK activation during ER stress therefore IRE1 α is a regulator in JNK activation (Urano, 2000). The cytoplasmic domain of IRE1 α binds TRAF2 adapter protein that couples plasma membrane receptors to cause JNK activation by stress-activated protein kinases (SAPKs) NH2-terminal kinases of which are a family of signal transduction proteins that are activated under a range of stimuli (Urano, 2000). JNKs regulate gene expression though a range of transcription factors cJUN ATF3 active components of anti-apoptotic activity (Urano, 2000). Deletion of TRAF2 inhibits JNK activation by TNF, TRAFs appear to be specifically important in the activation of kinase cascade culminating in JNK phosphorylation (Urano, 2000). The IRE1 α -mediated apoptosis therefore requires both IRE1 α kinase activity and AK1/TRAF2 interaction for ER stress mediated apoptosis.

1.8 IRE1 α Fv2E-Chimera

As discussed in section 1.1 cells have the ability to respond to endoplasmic reticulum stress through three upstream signalling proteins in multicellular eukaryotes (Han et al., 2009). For this project, we wish to investigate IRE1 α as this protein has a conserved counterpart in yeast while yeast has no known counterpart protein for AFT6 or PERK (Korennykh et al., 2011). Investigation into the function of IRE1 α has often been done through yeast HAC1. As yeast does not possess ATF6 or PERK, HAC1 can be activated in isolation to study its effects (Korennykh et al., 2011). Although ER stress can artificially be triggered in the lab by alteration in calcium stores in ER lumen or disturbance to the redox balance. Disturbances using these methods would also cause the activation of ATF6 and PERK (Ron and Walter, 2007).

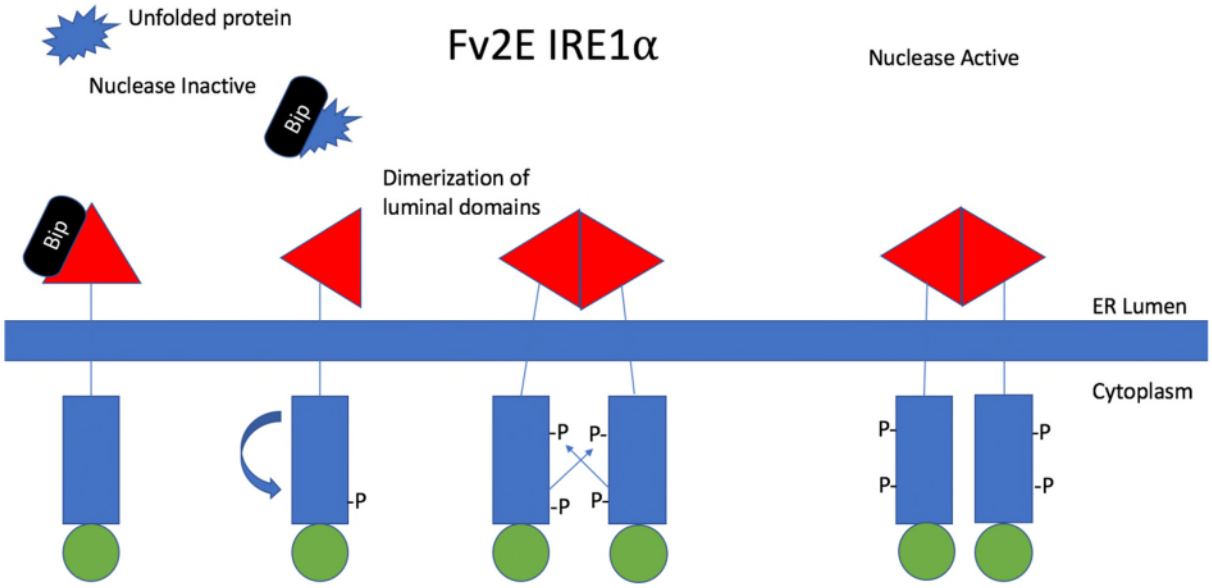

Figure 1.8.1, Activation of IRE1 α through activation Bip in response to unfolded proteins. Bip binds to unfolded protein and interacts with IRE1 α luminal domain. The Bip – IRE1 α interaction results in dimerization of IRE1 α cytoplasmic domains resulting in the active IRE1 α dimer.

As described in Fig 1.8.1, IRE1 α naturally interacts with Bip in the presence of unfolded proteins. Dimerization of the luminal domains results in phosphorylation of the cytoplasmic domains. To explore IRE1 α activation in isolation IRE1 α Fv2E-chimera has been created.

The Fv2E system allows for ER stress activation specific to IRE1 α without the use of stress mimetic drugs (Lu et al., 2004a) (Spencer et al., 1993). Through the fusion of the ERN1 cytoplasmic effector domain to a polypeptide containing two FK506 binding domains shown in Fig 1.8.2, (iDimerize, Takara). This results in a soluble cytoplasmic protein that can dimerise in the presence of a synthetic small organic molecule AP20187. The Fv2E system has been used to study PERK signalling (Deng et al., 2004), and IRE1 α (Watson., 2017). The Fv2E IRE1 α mutant dimerization has been shown to be sufficient for XBP1 splicing in the absence of ER stress (Back et al., 2006). Watson 2017 PhD thesis produced a system that can specifically activate IRE1 α though AP20187. Through this system we hope to investigate the downstream effects of the IRE1 domains in isolation from ATF6 and PERK by causing dimerization of Fv2E IRE1 α through exposure to AP20187.

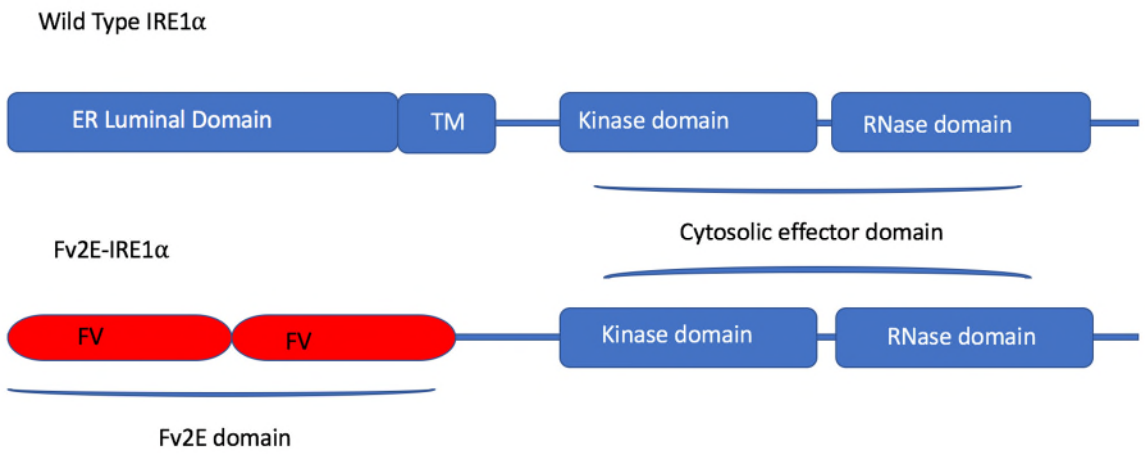

Figure 1.8.2, Comparison of wild type IRE1 α and Fv2E IRE1 α domains. The Fv2E mutant has the ER luminal and TM domains removed and replaced with two FK506 binding domains. This mutant is a soluble cytoplasmic protein that can dimerise in the presence of a synthetic small organic molecule AP20187

1.9 T-Rex™ mammalian expression system

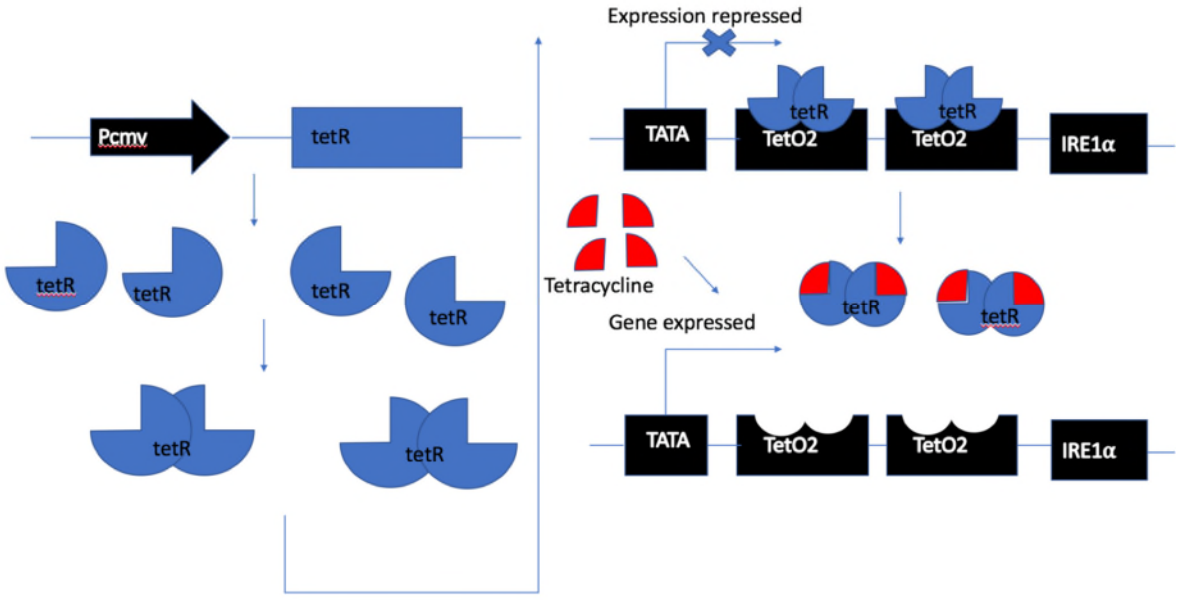

Figure 1.9.1, Diagram of T-REx induction of IRE1 α. Cells produce the protein TetR from the TetR gene. TetR forms a dimer and binds to TetO2 sequence downstream of TATA box and upstream of IRE1 α. Tetracycline introduced into the medium binds to TetR dimer, tetracycline prevents the binding of TetR to the Tet02 binding sites resulting in the gene being expressed.

The *IRE1 α* gene (*ERN1*) was cloned into multiple cloning sites of the inducible expression vector. The plasmid is co-transfected with a regulatory plasmid (pOG44) into mammalian cells. After transfection cells treated with tetracycline induce transcription of the gene of interest. The T-REx™ system allows tetracycline regulated expression in mammalian cells using regulatory elements from the *E. coli* Tn10-encoded tetracycline (Tet) resistance operon (Hillen and Berens, 1994; Hillen et al., 1983). In this system tetracycline binds to the Tet repressor and depresses the promoter controlling expression of the gene of interest

(Yao et al., 1998).

Using this system *IRE1 α* gene will be repressed in the absence of tetracycline and induced in the presence of tetracycline. Expression of the *IRE1 α* gene is controlled by the CMV promoter (Andersson et al., 1989; Boshart et al., 1985; Nelson et al., 1987). The promotor is next to two tet operator 2 (TetO2) inserted in tandem. In the absence of tetracycline, the repressor forms a homodimer with high affinity to the TetO2 sequences. Binding of the Tet repressor homodimers to TetO2 represses *IRE1 α*; tetracycline binds to Tet repressor homodimer causing conformation change rendering it unable to bind to Tet operator. The Tet repressor complex dissociates from the tet operated allowing induction and transcription for the *IRE1 α* gene as detailed in Figure 1.9.1.

1.10 Project objectives

This project explored the kinase domain of IRE1 α and if the kinase domain alone controls apoptotic cell death. To do this we attempted to create an RNase deficient kinase active Fv2E IRE1 α mutant. The project explored the domain activity of three IRE1 α mutants created as part of a Watson, Jamie, Nicholas (2017) PhD thesis. We also attempted to create new IRE1 α mutants based on mutations from Tirasophon et al., 2000.

We confirmed mutant IRE1 α expression using the T-REx^{tm} system and Western blotting of cell lysate as described in 1.9. We investigated if these mutations have lost the RNase activity of IRE1 α through the cleavage of XBP1. We extracted RNA before converting it to cDNA using XBP1 primers and running it on an agarose gel for visualisation under ultraviolet light. To do this we used the wild type Fv2E IRE1 α to determine the timeframe of XBP1 splicing before using the splicing assay to determine the RNase activity of each mutant. For mutants that no longer show RNase activity through XBP1 splicing assay, we explored kinase activity through Western blotting using the T-REx and Fv2E systems.

Mutants created that were kinase active and RNase deficient, were tested to confirm apoptotic capability through an MTT test for cell viability when compared to WT Fv2E IRE1 α. To define the activity of IRE1 α kinase activity we explored markers for cell death through apoptosis like PARP-1 and P-JNK.

2. Materials

2.1 Materials

The following section lists all materials used for experimentation in this thesis. Solutions are prepared in type I laboratory H2O (resistivity 18 MΩ cm, total organic carbon < 1 ppb, microorganisms < 1 cfu/ml, particles < 0.05 µm diameter) generated by the NANOpure Diamond UV/UF TOC water purification system and sterilized by autoclaving (121°C, 20 – 30 min).

2.2 Oligodeoxynucleotides for Homo sapiens genes

Table 2.2 Oligodeoxynucleotides

Name	Purpose	Sequence
H9406	Forward D847A mutation + BssHII cut site	CAGGGATTCCTTTTCTATTC**GCGCGC**TCACGTCCTGGAAGAAC
H9407	Reverse D847A + BssHII cut site	GTTCTTCCAGGACGTGA**GCGCGC**GAATAGAAAAGGAATCCCTG
H9408	Forward G923A mutation + Nhe1 cut site	TCGGGGAGGGAC**GCTAGC**GTCTCCCGC
H9409	Reverse G923A mutation + Nhe1 cut site	GCGGGAGAC**GCTAGC**GTCCCTCCCCGA
H9410	Forward D927A mutation + Sac2 cut site	AGCACACGAAGT**CCGCGG**GGAGGGACCC
H9411	Reverse D927A + Sac2 cut site	GGGTCCCTCC**CCGCGG**ACTTCGTGTGCT
H9412	Forward Y932A + NsbI cut site	GGGAAGCGAGACGTGAA**TGCGCA**CACGAAGTCGTCGG
H9413	Reverse Y932A + NsbI cut site	CCGACGACTTCGTG**TGCGCA**TTCACGTCTCGCTTCCC
3245L	XBP1-probe, 5'	CTGCTGATTCTTTGTCAGCG
3246L	XBP1-probe, 3'	TAGCATTAACAGTGACACGG

2.3 Antibodies for Western blotting

Table 2.3 Antibodies

Name	Primary / secondary	Host	Polyclonal/Monoclonal	Source	Product Number
Anti-HA	Primary	Rabbit	Polyclonal	Sigma-Aldrich	H6908
anti-IRE1 α	Primary	Rabbit	Polyclonal	Abcam	ab37073
anti-IRE1 α , phospho-S724	Primary	Rabbit	Monoclonal [EPR5253]	Abcam	ab124945
anti-JNK, phospho-T183/Y185	Primary	Rabbit	Monoclonal [81E11]	Cell Signalling	4668S
anti-PARP1	Primary	Rabbit	Polyclonal	Cell Signalling	9542S
anti-HA	Primary	Mouse	Monoclonal [12CA5]	Roche	1583816
Normal mouse IgG	Secondary	Mouse	Polyclonal	Santa Cruz Biotechnology	sc-2025
Normal rabbit IgG	Secondary	Rabbit	Polyclonal	Santa Cruz Biotechnology	sc-2027

2.4 Mammalian cell lines

Table 2.4 Mammalian cell lines

Name	Obtained from	Culture medium
Flp-In T-REx HEK 293. Human embryonic kidney	M. Cann, Durham University	DMEM, 10% FBS, 2 mM L-glutamine
Flp-In T-REx HEK293 with Fv2E-IRE1 α (K599A)stably integrated	Dr. David Cox, Durham University	DMEM, 10% FBS, 2 mM L-glutamine + 15 µg/ml blasticidin + 100 µg/ml hygromycin B
Flp-In T-REx HEK293 with Fv2E-IRE1 α stably integrated	Dr. David Cox, Durham University	DMEM, 10% FBS, 2 mM L-glutamine + 15 µg/ml blasticidin + 100 µg/ml hygromycin B

2.5 Cell culture reagents for tissue culture

Table 2.5 Cell culture reagents

Name	Supplier	Product number
Minimal essential medium	Sigma Aldrich	M2279
Dulbecco's modified Eagle's medium with pyruvate	Sigma Aldrich	D6546
Dulbecco's modified Eagle's medium without pyruvate	Sigma Aldrich	D5671
Fetal bovine serum	Biosera, Boussens, France	S1830
200 mM L-Glutamine solution	Sigma Aldrich	G7513
Penicillin (10000 U/ml)/streptomycin(10 mg/ml)	Sigma Aldrich	P4333
Trypan blue solution 0.4% (w/v) in 0.81% sodium chloride and 0.06% potassium phosphate.	Sigma Aldrich	T8154
Trypsin 0.25% (w/v)	Life Technologies Ltd	25200- 056
Hygromycin B (50 mg/mL)	Thermofisher scientific	10687010
Tetracycline hydrochloride	Sigma Aldrich	T7660
Blasticidin S HCl (10 mg/mL)	Thermofisher scientific	A1113902
AP20187	Clontech	635058

2.6 Reagents

Table 2.6 General use reagents

Name	Product Number	Company
5x First strand buffer	Y02321	Thermo Fisher Scientific
5x green GoTaq Flexi buffer	M891A	Promega
Acetic acid (HOAc)	A/0360/PB17	Thermo Fisher Scientific
Agarose	MB1200	Melford, Ipswich, UK
Ampicillin	BIA0104	Apollo Scientific,
β-Mercaptoethanol	M-6250	Sigma-Aldrich
Bovine serum albumin	A2153-50G	Sigma-Aldrich
Complete mini protease inhibitors	11836 153 001	Roche
D-Glucose	G/0500/61	Thermo Fisher Scientific
Ethidium bromide	E1510-10ML	Sigma-Aldrich
Glycerol	G/0650/17	Thermo Fisher Scientific
GoTaq Hot Start Polymerase 5 u/µl	M5001	Promega
GoTaq G2 flexi polymerase 5 u/µl	M7801	Promega
Glycine	BP381-1	Thermo Fisher Scientific
LB-Agar LENNOX	LBX0202	Formedium, King's Lynn,

		UK
LB-Broth LENNOX	LBX0102	Formedium
Methanol	M/4000/PC17	Thermo Fisher Scientific
Oligo(dT)15 500 µg/ml	C1101	Promega
PhosSTOP	4906837001	Roche
Propan-2-ol	P/7490/17	Thermo Fisher Scientific
RNasin Ribonuclease Inhibitor 20-40 u/µl	N22111	Promega
Tris(hydroxymethyl) methylamine (Tris)	T/3710/60	Thermo Fisher Scientific
Tween20	P1379-500	Sigma-Aldrich
Tetracycline	87130	Sigma-Aldrich

2.7 Special consumables

Table 2.7 Special consumables

Name	**Product Number**	**Company**
6-well plate, adherent	83.1839	Sarstedt, Nümbrecht, Germany
Polyvinylidene difluoride (PVDF) Transfer Membrane (0.45µm pore size)	RPN303F	GE Healthcare
CL-X Posure film	34091	Thermo Fisher Scientific
Tissue culture dish 58 cm2 Adherent	83.1802	Sarstedt
Tissue culture flask 175 cm2 Adherent	83.1812	Sarstedt
Tissue culture flask 75 cm2 Adherent	83.1811	Sarstedt
Tissue culture flask 25 cm2 Adherent	83.181	Sarstedt
Tissue culture flask 175 cm2 Suspension	83.1812.502	Sarstedt
Tissue culture flask 75 cm2 Suspension	83.1811.502	Sarstedt
Tissue culture flask 25 cm2 Suspension	83.1810.502	Sarstedt
Microtest Plate 96 Well,F	82.1581.001	Sarstedt

2.8 Commercially available kits

Table 2.8 Commercially available kits

Name	Product Number	Company
GenElute plasmid mini prep kit	PLN10	Sigma-Aldrich
QuikChange II XL Site-Directed Mutagenesis Kit	200521	Agilent Technologies
Amersham ECLTM Western blotting detecting reagents	RPN2009	GE Healthcare, Buckinghamshire, UK
DCTM Protein assay reagent A	500-0113	BIORAD
DCTM Protein assay reagent B	500-0114	BIORAD
DCTM Protein assay reagent S	500-0115	BIORAD
EZ-RNA kit (solution A and B)	K1-0120	Geneflow, Lichfield, UK
GeneRuler 1 kb DNA ladder	SM0311	Thermo Fisher Scientific
GeneRuler DNA ladder mix	SM0331	Thermo Fisher Scientific
GoTaq qPCR Master Mix	A6002	Promega, Southampton, UK
jetPRIME ® DNA Transfection Kit	114-07	Polyplus transfection, Illkirch, France
PageRuler Plus prestained protein ladder	26619	Thermo Fisher Scientific
Pierce ECL Western blotting substrate	32209	Thermo Fisher Scientific
Tetro cDNA synthesis kit	BIO-65042	Bioline, London, UK
GenElute High Performance (HP) Plasmid Maxiprep	NA0300	Sigma-Aldrich
Complete protease inhibitors	1.1836E+10	Roche, Basel, Switzerland

2.9 Growth media containing ampicillin

2.9.1 LB agar ampicillin plates

35 g of LB agar Lennox (Formedium) for every 1000 mL dH_2O and was mixed. The mixed medium was added to a flask, covered with foil and autoclaved. When the flask was cool, ampicillin at a 1:1000 dilution was added under sterile procedure to giving a concentration of 50 µg/ml. 25 ml of the solution was plated on to petri dishes(SLS 9CM Petri dish single vent) using sterile procedure, when solid the petri dishes were wrapped with Para film, store at 4˚C. Dry LB plates in an incubator at 37˚C for 1 h or until dry.

2.9.2 LB agar broth

20 g LB broth was added for every 1000 ml dH_2O, mixed in a flask and autoclaved (prestige medical clinical autoclave 9 L). When the broth was cool, ampicillin was added at a 1:1000 dilution. Final concentration of the solution was 50 µg/ml.

2.10 Sequence analysis

Plasmid DNA sequences were sequenced by DBS Genomics Durham and analysed using SnapGene software version or 3.0.3 pDRAW32 revision 1.1.131.

2.11 Sterilisation of equipment

Solutions and glassware were autoclaved at 121°C for 20 min and 1 atmosphere.

3 Methods

3.1 Bacterial culture

All work with *E. coli* was carried out beneath a Bunsen burner flame on a bench that had been sterilised with 70 % (v/v) ethanol. The orifices of any tubes, flasks or bottles that were opened during bacterial culture were flamed using the Bunsen burner before and after use.

3.1.1 Reviving bacterial cultures

Cultures were removed from -80˚C, a small sample was chipped from the frozen stock using a sterile pipet on to a LB agar ampicillin plate (2.9.1) Bacteria were spread on LB agar plate using sterile procedure, incubate overnight in 37˚C.

3.1.2 Growth of *E. coli* Cultures

4 ml LB-broth containing the appropriate concentration of antibiotics to select for the desired bacteria were inoculated with cells from a single *E. coli* colony. The *E. coli* were incubated at 37 ºC with shaking at 225 – 250 rpm overnight. The cells were collected by centrifugation at 12,000 g for 1 min at room temperature and washed three times with 1 ml of LB-broth. The pellets were resuspended in LB broth and diluted 1:100 into LB-broth containing the appropriate concentration of antibiotics. Cultures were incubated at 37 ºC with shaking at 225 – 250 rpm overnight.

3.1.3 Snap freezing bacterial cultures

1 ml of 30 % (v/v) glycerol was mixed with 1 ml of fresh overnight culture in a 2 ml cryo-vial and flash-frozen in liquid nitrogen before storage at -80 ˚C.

3.2 Protocols for the preparation/use of DNA

3.2.1 PCR primer design

Site directed mutagenesis was applied using polymerase chain reaction (PCR) and QuickChange Lightning Multi Site-Directed Mutagenesis Kit from Agilent Technologies. QuickChange primers were designed on Agilent website and then synthesised by Eurogentec. (For primer sequences see materials), primers were dissolved in double distilled water to a concentration of 100 µM and stored at -20˚C.

3.2.2 Plasmid concentration analysis

Concentrations was measured using a NanoDrop ND-1000 spectrophotometer and ND-1000 software version 3.2.1. Protocol specific for this machine can be found on the manufacturer's website.

Or concentrations were measured using SpectraMax 190 Microplate Reader and softmax pro software with a wavelength of 260 nm. 1 µl of plasmid was added to 49 µl if dH_2O into a microplate. The plate was read by the SpectraMax 190 Microplate reader against a control of sterilised water.

3.2.3 DNA Agarose Gel Electrophoresis

0.3-3.0 g of electrophoresis-grade agarose were placed into an Erlenmeyer flask along with 30-150 ml of TAE buffer and melted with heating. The DNA samples were mixed with 6x DNA loading dye and added to the wells alongside a *GeneRuler* DNA ladder. The gel was run at 120 V and the DNA was visualized at 312 nm, 0.120 J/cm^2 using a UV transilluminator.

3.2.4 Preparation of ultracompetent XL10-Gold Cells

The XL10-Gold cells (Agilent Technologies) were removed from storage at -80˚C and slowly thawed in ice and 35 µl of cells were aliquoted into cooled 1.5 ml microcentrifuge tubes. Once thawed on ice 1.5 µl XL 10-Gold ß-Mercaptoethanol (ß-ME) was added and mix (Agilent Technologies). The mixture was gently swirled every two min for ten min while still on ice.

3.2.5 QuickChange Lightning Multi Site-Directed Mutagenesis PCR

16.75 µl double-distilled H2O was added to a test tube. To this mixture the following regents were added, 2.5 µl 10x Quickchange Lightning Multi reaction buffer, 0.75 µl Quicksolution, 1 µl of diluted ds-DNA template, 1 µl of each diluted mutagenic primer, 1 µl dNTP mix, 1 µl QuickChange Lightning Multi enzyme blend. The complete reaction mixture was placed in a PCR thermal cycler, and used these modified thermal cycling parameters.

Reaction rates

Initial denaturation	95.0°C	2 min	
Denaturation	95.0°C	20 s	
Annealing	55.0°C	30 s	x 30 cycles
Extension	65.0°C	3.5 min	
Final extension	65.0°C	5 min	
Hold	4.0°C	∞	

The cycler maintained temperature at 5˚C until sample was removed for storage.
Once PCR reaction was complete, the product was cooled on ice and then stored at -20˚C.

3.2.6 Digestion of methylated parental DNA

The cooled quick-change PCR product had 1.5 µl of *DpnI* restriction enzyme (Agilent Technologies) added directly to the thin-wall PCR tube. PCR product was placed in a incubator for 10 min at 37 ˚C, the digested PCR product was stored at -20 ˚C.

3.2.7 Introduction of plasmid to XL10-Gold cells

Introduction followed modified manufactures protocol, (http://www.agilent.com/cs/library/usermanuals/Public/200314.pdf) modification below.

The PCR tube was removed from the incubator, 5 µl of the digested plasmid was added gently but directly to the Eppendorf tube containing 35 µl of XL10-Gold cells. The mixture was incubated on ice for thirty minutes, during this incubation a water bath was heated to 42 ˚C, after incubation finished the Eppendorf tube was heat shocked for 30 seconds in the water bath then put back on to ice for two minutes.

500 µl of SOC medium (2.13) was added to the transformed cells, the sample was incubated in an incubator at 37˚C and rotated at 220 rpm for an hour.

3.2.8 Plating transformed cells

The transformed cells were removed from the incubator, using aseptic technique 200 µl of cells was plated and spread on kanamycin selective LB agar plate (2.9.1). The plate was incubated overnight at 37˚C to allow growth of transformed colonies. The transformed culture of cells was stored at 4˚C and re-plated if no colonies formed.

3.2.9 Culturing bacteria

Colonies were selected using autoclaved tooth pick and sterilised forceps and placed into a bacterial culture tube and 4 ml LB ampicillin broth (2.9.2.), Incubate 37˚C 250rpm overnight (infors ht shaker). 1 ml of overnight culture was pelleted, supernatant was aspirated and discarded, the pellet was re-suspended in 1 ml of dH_2O. Pellet was washed in this way three times. Re-suspend pellet in sterile water and add to 100mL LB broth with 100 µl ampicillin (2.9.2.) in a 250 ml flask, incubate overnight at 37˚C 250 rpm (infors ht shaker).

The 100 ml overnight culture was decanted from its flask into 250 ml 8 oz centrifuge tubes (Nalgene) and placed on ice. The culture was pelleted in a Beckman coulter Avanti j-26 XP centrifuge at 4800 g 4˚C for 15 minutes with JLA 16.250 rotor. The supernatant was aspirated and discarded, the pellet was stored at -20˚C.

3.2.10 Plasmid DNA midiprep from *E. coli* (Sigma-Aldrich)

Plasmid DNA midipreps were carried out using Sigma's GenElute^{TM} HP Plasmid Midiprep Kit (2.8 Commercially available kits). Please refer to manufactures instructions for protocol.

3.2.11 Restriction analysis

Prepare on ice an Eppendorf tube containing, dH_2O to the final volume 20 µl, 500 ng plasmid DNA, 0.5 µl *BGLII* and 2µl of 10x buffer O. The tube was incubated 37˚C for one hour in a water bath. The mixture was electrophoresed on an agarose gel as described in 3.2.3. The gel was loaded with 5 µl GeneRuler 1 kb DNA ladder (Thermo Scientific), 20 µl of each digested plasmid + 4 µl 6X loading dye (thermo scientific) and 1 µl of each undigested plasmid mixed with 4 µl water and 1 µl dye (Thermo Scientific). The DNA was then visualized at 312 nm, 0.120 J/cm^2 using a UV transilluminator.

3.3 Protocols for mammalian cell experiments

3.3.1 Mammalian Cell Culture

All cell cultures were maintained in a medium of DMEM +10% FBS. Antibiotic resistant lines were cultured in DMEM, 10% FBS, 2 mM L-glutamine + 15 µg/ml blasticidin + 100 µg/ml hygromycin B (2.4). Cells were incubated at 37 °C with 5 % (v/v) CO_2 at 95 % humidity. All work was done in a laminar flow cabinet. Equipment, including the flow hood, was sterilised with 70 % (v/v) ethanol before use.

3.3.2 Reviving mammalian cells

Cells were removed from liquid nitrogen stores at -130˚C. Cells were thawed in 37˚C water bath. In a cell culture fume hood using sterile procedure cells were added to 9 ml DMEM + 10 % FBS + 2 mM L-Glutamine (100 µg/ml hygromycin B + 15 µg/ml blasticidin if appropriate) in an adherent culture flask. Cells were cultured at 37 °C with 5 % (v/v) CO_2 at 95 % humidity.

3.3.3 Cell Counting with a Haemocytometer

Cells were detached and resuspended in the appropriate medium as described above. A 100 µl sample of the cell suspension was aliquoted into a sterile 1.5 ml microcentrifuge tube and mixed in a 1:1 ratio with 0.4 % (v/v) trypan blue in 0.9 % (w/v) NaCl by gently pipetting up and down four times. The haemocytometer was cleaned using 70 % (v/v) ethanol and the cover slip was attached using a few droplets of water from a 10 ml pipette. ~ 10 µl of the cell suspension was loaded underneath the cover slip using the loading groove and left to settle for 2 min. The counting grids were visualised at a 100x magnification and the cells within a square of area 0.04 mm^2 were counted on both of the counting grids so that the average number of cells per ml of medium could be calculated using the following formula: Cells/ml = 2 x average count per square x dilution factor x 10^4.

3.3.4 Maintaining mammalian cell lines

Medium was removed from flask, cells were washed with 5ml PBS (Gibco) followed by 0.5 ml Trypsin-EDTA (Gibco) wash. The flask was placed into the incubator 37 °C with 5 % (v/v) CO_2 at 95 % humidity until cells detached, once loose cells were re-suspended in 10 ml

DMEM + 10 % FBS + 2 mM L-Glutamine. Cells were split into new in 75 cm_2 adherent cell flask with fresh medium (100 µg/ml hygromycin B + 15 µg/ml blasticidin if appropriate) with a total volume of 10 ml.

3.3.5 Transfection of mammalian cells (jetPRIME®)

HEK 293 Flp-In Trex cells were split as described in 3.3.4 and counted as described in 3.3.3, 80,000 cells were plated into 2 ml medium in a 6 well plate and cultured overnight. In a sterilise Eppendorf tube add 500 µl jetPRIME ® buffer, add 2 µg of DNA at 9:1 ratio of pOG44 to desired plasmid DNA and 4 µl of jetPRIME® reagent. The Eppendorf tube was briefly vortexed and incubated for 10 min at room temperature. The contents were gently dropped onto the wells of the 6 well plate in the cell culture fume hood. Medium was replaced with medium containing 50 µg/ml hygromycin B for 2 d, then increased hygromycin B concentration to 100 µg/ml; maintain 15 µg/ml blasticidin throughout. Cells were incubated at 37 °C with 5 % (v/v) CO_2 at 95 % humidity.

3.3.6 RNA extraction (GeneFlow)

Cells were split as described in 3.3.4 and counted using 3.3.3. $1x10^6$ cells were seeded into 10 cm culture dish, Cultured overnight at 37 °C with 5 % (v/v) CO_2 at 95 % humidity.

We used EZ RNA kit (Bioind) to extract RNA following the manufacture protocol (http://www.bioind.com/ez-rna-total-rna-isolation-kit/).

We removed the medium and wash with room temperature PBS. We lysed the cells directly to culture dish using 0.5 ml denaturing solution. The cells were scraped off and collected in an Eppendorf tube and 0.5 ml extraction solution were added. The mixture was shaken for 15 min and stored at room temperature for 5 min. Centrifuge at 12,000 g for 15 min at 4˚C. Transfer upper phase to fresh tube. Add 0.5ml ice cold isopropanol per 0.5 ml denaturing solution. Invert tube 5 times. Store overnight at -20˚C to increase yield. Centrifuge for 30 min at 4˚C 12,000 g. Aspirate supernatant. Add 1 ml ice-cold 75 % ethanol (v/v) votex briefly. Centrifuge 15 min at 4˚C and 12,000 g. Aspirate supernatant. Centrifuge tubes at 4˚C, 12,000 g for 10-15 s and aspirate supernatant. Air-dry pellet for 5 min. Dissolve pellet in 20 µl DEPC H_2O. Store at -80˚C.

3.3.7 cDNA synthesis

To produce cDNA we followed Tetro cDNA synthesis kit protocol. (https://www.bioline.com/au/tetro-cdna-synthesis-kit.html)

3.3.8 XBP1 Splicing assay

In a sterile, nuclease free PCR tube 19 µl H_2O was added, to this test tube the following reagents were added, 10 µl 5 x Green GoTaq flexi buffer, 3 µl 25 mM $MgCl_2$, 5 µl 2 mM dNTPs in 1 mM Tris·HCl, pH 8.0, 5 µl 10 µM forward primer F2, 5 µl 10 µM reverse primer R2, 2.5 µl cDNA from above and 0.5 µl 5 U/µl GoTaq hot start polymerase.

The following cycling parameters were used:

Initial denaturation	94.0°C	2 min	
Denaturation	94.0°C	1 min	
Annealing	59.0°C	1 min	x 35 cycles
Extension	72.0°C	30 s	
Final extension	72.0°C	5 min	
Hold	4.0°C	∞	

The whole 50 µl reaction was electrophoresed at 100 V for 1 h on a 2 % (w/v) agarose gel with 1x TAE as a running buffer containing 1 µg/ml ethidium bromide (p018). The Bands were visualised under UV.

3.3.9 MTT assay for cell viability (Mosmann, 1983)

To assess the number of living cells post-treatment an MTT (3-[4,5-Dimethylthiazol-2-yl]-2,5-diphenyltetrazolium bromide; Thiazolyl blue) colorimetric assay was used. ~80,000 cells were seeded in 9 ml DMEM + 10 % FBS + 2 mM L-Glutamine 100 µg/ml hygromycin B + 15 µg/ml blasticidin.100 µl was seeded into the cavities of a 96 well tissue culture plate and left overnight (20% confluency). Cells were treated with 1 µg/ml tetracycline, 200 nM AP20187, for 48 h. After the desired treatments had concluded, the medium was aspirated and replaced with fresh DMEM medium that lacked phenol red, but contained 0.5 mg/ml MTT. The cells were incubated at 37 °C with 5 % (v/v) CO_2 at 95 % humidity for 3 h. The medium was aspirated and replaced with 150 µl of 4 mM HCl, 0.1% (v/v) Nonidet P-40 in isopropanol. The plates were covered with aluminium foil and shaken for 15 min on an orbital shaker at room temperature to dissolve the MTT crystals. Once this was done the absorbance was read at 590 nm and 690 nm (reference wavelength) using a microplate reader.

3.3.10 Protein isolation from mammalian cell lines

$5x10^6$ Cells were seeded as described in 3.3.4 into 9 cm adherent cell dishes. The dishes were incubated as described 3.3.1 overnight before treatment.

RIPA buffer was produced on the day of protein isolation as described in (2.9). One *PhosSTOP* phosphatase inhibitor (Roche) and one *Complete mini protease inhibitor cocktail* tablet (Roche) were added to 10 ml of ice-cold RIPA buffer. The RIPA buffer containing containing complete protease inhibitors and phosphatase inhibitors was prepaired fresh on the day of isolation as the inhibitors are only stable for 24 h once dissolved.

The cells were placed on ice and the medium was aspirated and discarded. The cells were washed three times in 2 ml of ice-cold PBS before the addition 300 µl of ice-cold RIPA buffer. The cells were scraped in order to detach them from the dish. The dishes were left at an angle of ~45° for 5 min on ice to ensure all of the cells had been collected before being transferred to a 1.5 ml microcentrifuge tube and incubated for 10 min on ice to allow lysis to occur. The protein lysates were centrifuged at 16,000 g for 10 min at 4 °C to pellet the cell debris and the supernatants were transferred to fresh 1.5 ml microcentrifuge tubes.

3.3.11 Bio-Rad DC Protein assay

Protein sample was diluted 1:10 in dH_2O. Pipette 5 µl sample, standard including the blank, and buffer control into a clean, dry microtiter plate with two repeats for all samples. The buffer control is RIPA buffer diluted 1:10 in H_2O. 25 µl Bio-Rad reagent A and 200 µl of Bio-Rad reagent B into each well using a multichannel pipette. The microtiter plate was incubated at RT for 15 min with gentle shaking. Read absorbance at 750 nm in a microplate reader (molecular devices spectramax 190).

3.4 Western blotting

3.4.1 Protein electrophoresis

Protein was isolated and concentration was measured as described in (2.2.20). We combined 20-30 µg of protein with 6x SDS-PAGE loading buffer and denatured at 70 °C for 10 min before being separated by gel electrophoresis.

The electrophoresis unit was disassembled, the glass was washed in 10% sds followed by 70 % ethanol. The glass slides were inserted and the unit was reassembled on a rubber base to prevent gel leakage.

The following mixture was used to create a 10 % separating gel. All reagents were prepared on ice and degassed for 5 min during the stages below.

Table 3.4.1.1 Separating gel mix

Component	Volume
30 % (w/v) acrylamide, 0.8% (w/v) bisacrylamide	2.50 ml
1 M Tris·HCl, pH 8.9	1.875 ml
H_2O	3.13 ml
Add after degasing:	
10 % (w/v) SDS	50 µl
10 % (w/v) ammonium persulfate	45 µl
TEMED	10 µl
Total	7.61 ml

Table 3.4.1.2 Stacking gel mix

Component	Volume
30 % (w/v) acrylamide, 0.8 % (w/v) bisacrylamide	0.34 ml
1 M Tris·HCl, pH 6.8	0.625 ml
H_2O	1.56375 ml
Add after degasing:	
10 % (w/v) SDS	6.25 µl
10 % (w/v) ammonium persulfate	22.5 µl

TEMED	7.5 µl
Total	2.56 ml

5 µl of page ruler (thermo scientific) was added to the first well of the gel. 20-30 µg of total protein + 6x SDS-PAGE loading buffer of each protein sample was pipetted into each well. The gel was left to run for 1 h at 120V.

3.4.2 Membrane semidry transfer

The SDS-PAGE gel was removed from its casing and carefully transferred to a plastic container containing 1x Semi-dry Transfer Buffer (2.9) and then incubated with gentle shaking for 30 min.

PDVF membrane was washed in methanol for 1 min and then incubated with gentle shaking for 30 min in 1x Semi-dry Transfer Buffer (2.9). 8 pieces of Whatman 3 MM paper were incubated with gentle shaking for 30 min 1x Semi-dry Transfer Buffer (2.9). The SDS-PAGE gel & PDVF membrane was placed between 8 pieces of incubated Whatman 3 MM paper.

The surface of the anode of the semi-dry transfer unit was cleaned before assembly of the gel stack. 4 of the pre-soaked pieces of Whatman 3 MM paper where placed in a neat stack on the semi-dry transfer apparatus, a 50 ml tube was then rolled over the stack to remove bubbles. The incubated PDVF membrane was placed upon this stack and then the SDS gel was placed on top of the membrane. The remaining 4 pieces of incubated Whatman 3 MM paper were stacked on top of the gel. A 50 ml tube was rolled over the stack gently to remove bubbles. The apparatus was then set to transfer at 2 mA/cm2 for 60-75 min.

The membrane was stored at 4°C in a 50 ml falcon tube filled with TBST (2.9).

3.4.3 Antibody staining

The membrane was blocked overnight with bovine serum albumin BSA 5 % (v/w) (2.9) in 4°C cold lab or for one hour at room temperature. The membrane was washed three times in Tris-buffered saline + Tween 20 TBST (2.9), then incubate in 3 ml BSA 5 % and 3 µl antibody (2.3), BSA was necessary for blotting of phosphorylated proteins. The membrane was washed in TBST for 5 min three times, then incubated in 5 % milk with a secondary antibody at a 1:1000 dilution.

3.4.4 Chemiluminescence detection with luminol

The following mixture was prepared immediately before use and kept protected from light:

15 ml 100 mM Tris-HCL, pH 8.5 + 0.1 % (v/v) Tween 20
75 µl 250 mM luminal
33.3 µl 90 mM p-coumaric acid
4.35 µl 30 % (w/w) H_2O_2

This was mixed well and protected from light.

The membrane was washed again in TBST for 5 min three times. The membrane was gently dried and place in an X-ray cassette inside of a plastic cover.

The following steps were performed in a dark room.

1 ml of the above solution was pipetted onto the membrane. The membrane was incubated for 1 min at RT in the dark. A photographic film was placed on top of the plastic cover and membrane inside the X-ray cassette. The X-ray cassette was closed and left to expose for 0.5-5 min. The exposed film was removed from the cassette and developed in X-ray film processor (Compact X4 Automatic Processor).

3.4.5 Immunoprecipitation

Prior to protein isolation, phosphatase and protease inhibitors (Roche) were added to the RIPA buffer as described in section (3.3.10)

Pre-clearing: 20 µl of Protein A-agarose beads (2.9) were centrifuged at 100 g for 2 min. The supernatant was pipetted and removed, the beads were then re-suspended in 100 µl of RIPA buffer before being centrifuged at 800 rpm for 2 min. The supernatant was pipetted and discarded.

To the pre-cleared protein A-agarose beads, 250 µg of protein dissolved in 200 µl of RIPA buffer was added and 0.8 µg of rabbit IgG. The samples were incubated at 4 ^{o}C for 1 h whilst rotating at 8 rpm (Stuart rotator drive STR4). The samples were then centrifuged at 800 rpm for 2 min before the supernatants were transferred to fresh 1.5 ml micro-centrifuge tubes. 5 µl of antibody specific to the protein (anti-HA) (2.3) that was being used as the "bait" during the assay were added to the samples and incubated overnight at 4 ^{o}C rotating at 8 rpm. 20 µl of protein A-agarose beads were added to the protein lysates and incubated for 1 h at 4 ^{o} C whilst rotating at 8 rpm. The samples were centrifuged at 800 rpm for 2 min before the supernatants were discarded. The beads were subjected to three washes in 500 µl RIPA buffer + 0.1% NP-40. 500µl RIPA buffer were added to the protein A-agarose beads and centrifuged at 800 rpm for 2 min before the buffer was discarded. The protein A-agarose beads were centrifuged a final time for 2 min at 800 rpm and any residual buffer was removed. 30 µl of 6x SDS-PAGE sample buffer were added to the beads, which were heated at 70 ^{o}C for 10 min. After this, the samples were collected via centrifugation for 15 s. The proteins were then separated by electrophoresis and analysed by Western blotting as described in (3.4.1-3.4.4).

4. Results

4.1 Introduction

As discussed in the introduction, IRE1 α controls cell survival or apoptosis during endoplasmic reticulum stress. Given the important role of IRE1 α in cell fate it represents an important target for therapeutic intervention in pathogenic diabetes, cancer and other UPR-related diseases. It is possible that IRE1 α functions are separated between its RNase and Kinase domains. IRE1 α protective and apoptotic signalling could be controlled through two distinct enzymatic domains. Inhibition of the Kinase domain whilst retaining the functioning RNase domain could result in only protective cell signalling preventing apoptosis. This hypothesis of IRE1 α domain roles means that protective signalling would only be therapeutic if the Kinase domain alone signalled apoptotic cell death.

Therefore, it was decided to investigate the activity of the Kinase domain by characterising a kinase active RNase deficient Fv2E IRE1 α mutant. To investigate this possibility, I used an Fv2E IRE1 α mutant, and using site-directed mutagenesis to create point mutations in key RNase residues before transfecting into Flip-In T-REx HEK293 cells to be transcribed and translated.

As discussed in the introduction I plan on using an Fv2E chimera to cause IRE1 α activation in insolation from ATF6 and PERK. Alongside this system I plan to transfect our mutants into Flip-in T-REx cells. Flip-in cells contain a stably integrated FRT site at a transcriptionally active genomic locus (Thermofisher.com, 2018), this will allow the generation of stable cell lines that can express the Fv2E IRE1 α in high levels (Thermofisher.com, 2018). Although this expression is desirable overexpression could result in the unintentional activation of our mutant, because of this I will control the gene expression though T-REx system (Thermofisher.com, 2018) as described in Figure 1.9.1. Flip-in T-REx Hek 293 cell lines have shown low basal expression of the target gene in control samples, while in the presence of tetracycline show high expression of the target gene (Thermofisher.com, 2018)

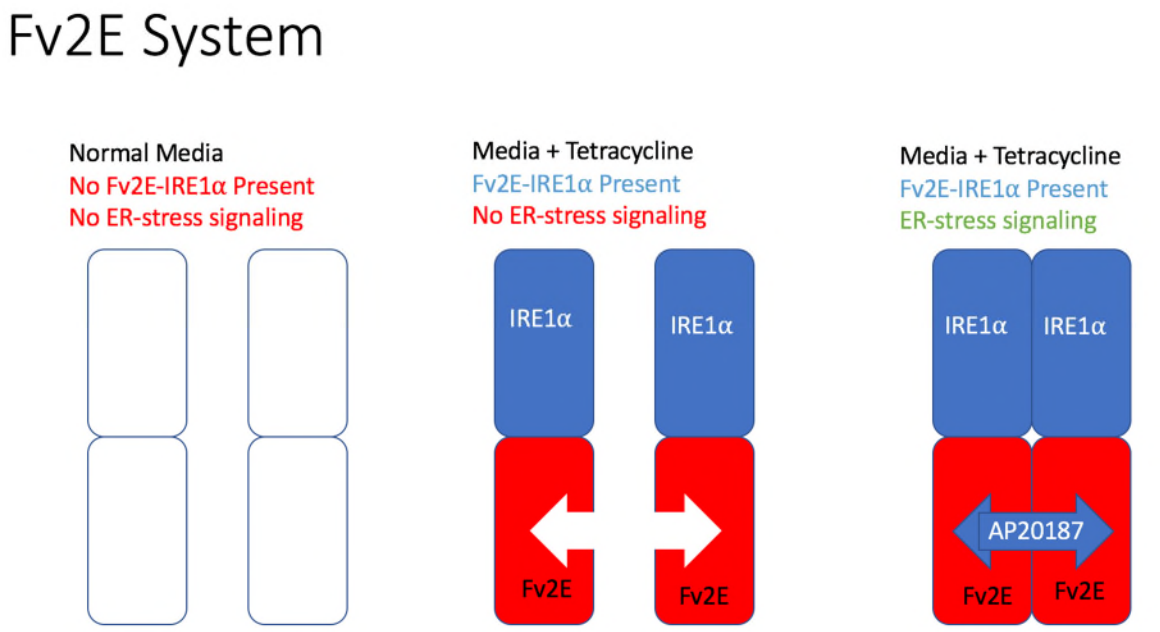

Figure 4.1.1, Diagram of Fv2E IRE1 α in media containing tetracycline or tetracycline and AP20187 (B-B homodimer). Normal media should have very low expression of IRE1 α and no dimerization of IRE1 α. Media containing tetracycline should overexpress the Fv2E IRE1 α mutant with little to no dimerization. In media containing tetracycline and AP20187 (B-B homodimer) should overexpress Fv2E IRE1α and dimerise resulting in P-IRE1 α. In WT IRE1 α dimerization occurs in the presence of unfolded protein. AP20187 will cause dimerization of the luminal domains of the Fv2E IRE1α mutant as seen in WT cells under ER stress.

As described in Figure 4.1.1, our test will involve two treatments and a control for each mutant. By testing the three samples I will be able to determine if cell viability is affected by the tetracycline treatment, or the overexpression of the Fv2E IRE1 α mutant induction by tetracycline treatment. By comparing the results from control, tetracycline and tetracycline + AP20187 (B-B homodimer) I hope to be able to characterise the mutations to IRE1 α mitigating the possible effects of tetracycline and AP20187 on the results.

By characterising a Kinase active RNase deficient mutant to discern if the kinase domain alone is capable of causing apoptosis. If this is possible then it would indicate that the two enzymatic domain functions are distinct and that the TRAF2 apoptotic signalling does not require influence from the RNase domain.

4.2 Expression of Fv2E *IRE1 α* in Flip-in T-REx HEK 293 cell lines

Three other Fv2E *IRE1 α* mutants (K907A, N906A and H910N) had already been created and acquired for this project, these mutations in yeast caused Kinase active RNase deficient mutants (Tirasophon, 2000) and therefore were chosen given the high likelihood of producing the desired characterises in mammalian cells. We extracted the plasmids from *E. coli* using the protocol from (3.2.10) and transfected in to Flp-In T-Rex HEK293 cells using (3.3.5) protocol. We tested the three mutants for expression of Fv2E *IRE1 α* and used two control cell cultures WT and K599A Fv2E IRE1 α. K599A Fv2E IRE1 α is a mutant that stably produced in HEK 293 cell that are Kinase and RNase dead. The three mutant cultures and two control cultures were split as described in (3.3.4) using sterile technique.

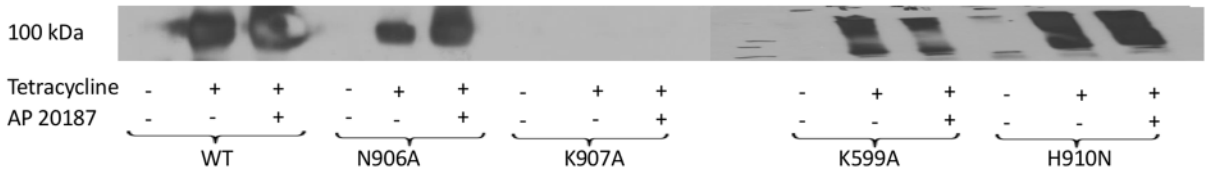

Figure 4.2.1, Flp-In T-Rex HEK293 Fv2E-IRE1α mutants were treated with tetracycline (1 µg/ml) and AP20187 (200 nM) for 48 h. Cells were lysed and lysate was extracted as described in (3.3.10) for Western blotting. Cell lysate was Western blotted as described in (3.4) with anti-HA antibody on two separate Western blots.

Through Western blotting we confirmed successful transfection of HEK 293 cells with Fv2E *IRE1 α* N906A and H910N as seen in Figure 4.2.1. We noted that the K906A Fv2E *IRE1 α* mutant culture although antibiotic resistant did not produce protein upon exposure of tetracycline. Sequencing of the *Fv2E IRE1 α K907A* plasmid as described in (2.10) showed that the sequence differed from the WT *Fv2E IRE1 α* plasmid. Inspection of the *Fv2E IRE1 α* sequence map, revealed that the K907A mutant plasmid did not contain the Fv2E region required for expression of the protein.

4.3 RNase domain activity

The RNase domain of IRE1 α cleaves XBP1 and the ligase complex Rtc2B ligates the exons (Kosmaczewski et al., 2018) into its active form XBP1s for intracellular signalling (Tsuru et al., 2018), however we do not know how long this process takes. To determine the RNase activity of the Fv2E IRE1 α mutants we first determined the time frame for WT Fv2E IRE1 α XBP1 splicing to XBP1s through an XBP1 splicing assay as described in (3.3.8).

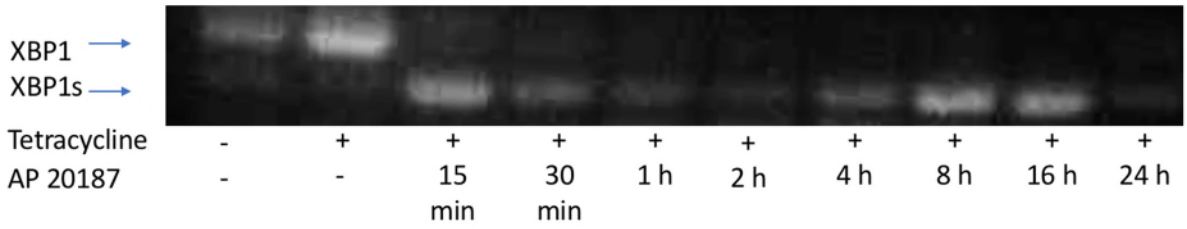

Figure 4.3.1, Flp-In T-Rex HEK293 Fv2E-IRE1 α WT was treated with tetracycline (1 µg/ml) for 24h before exposure to tetracycline (1 µg/ml) and AP20187 (200 nM) as described in above. RNA was extracted as described in (3.3.6) and transformed in to cDNA as described in (3.3.7). The RNA was tested through an XBP1 splicing assay explained in (3.3.8). No housekeeping control was used; therefore no numerical comparisons could be completed on this image.

It was noted that XBP1 splicing was seen within the first 15 minutes, and possibly earlier after exposure. For the testing of the three mutants a tetracycline (1 µg/ml) for 24 h before exposure to tetracycline (1 µg/ml) and AP20187 (200 nM) for 24h was chosen for maximum splicing. It was noted that the 24h time point likely shows reduced expressions due to cell death caused by IRE α activation by AP20187 leading to reduced protein present in tested samples.

I tested the RNase activity of the two Fv2E IRE1 α mutants and used two control cell cultures WT and K599A Fv2E IRE1 α. The three mutant cultures and two control cultures WT and K599A were split as described in (3.3.4) using sterile technique.

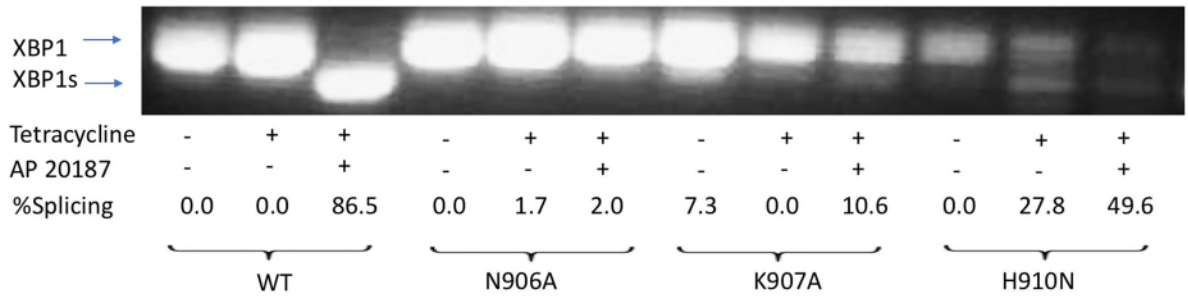

Figure 4.3.2, Flp-In T-Rex HEK293 Fv2E-IRE1 α mutants were treated with tetracycline (1 µg/ml) for 24h before exposure to tetracycline (1 µg/ml) and AP20187 (200 nM) for 24h. RNA was extracted as described in (3.3.6) and transformed in to cDNA as described in (3.3.7). The RNA was tested through an XBP1 splicing assay explained in (3.3.8). Analysis was performed using LI-COR image studio software.

As seen in Figure 4.3.2, XBP1 splicing is clearly visible in the WT Fv2E IRE1 α and partial splicing in the H910N mutant with 24h tetracycline and 24h tetracycline and AP20187 exposure. We noted that the N906A mutant did not have XBP1 Splicing. We decided that the H910N Fv2E IRE1 α mutant still retained RNase activity. We concluded that the N906A Fv2E IRE1 α mutant RNase splicing was repressed through the point mutations and proceeded to characterise its Kinase activity as seen in chapter 3.5.

4.4 Kinase activity

Of the three mutated plasmids tested, one culture possessed RNase dead Fv2E IRE1 α expression. We decided to test the kinase activity of the Fv2E IRE1 α N906A mutant against the Kinase activity of the WT Fv2E IRE1 α.

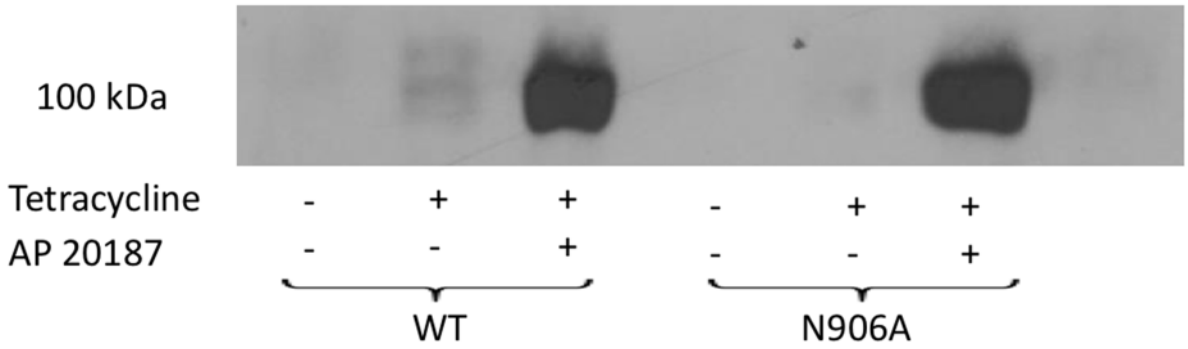

Figure 4.4.1, Flp-In T-Rex HEK293 Fv2E-IRE1 α WT and N906A were treated with tetracycline (1 µg/ml) and AP20187 (200 nM) for 48h. Cell lysate was extracted as described in (3.3.10) for Western blotting. Cell lysate was Western blotted as described in (3.4) with anti-p-IRE1 α (S724).

As can be seen the Western Blotting Figure 4.4.1, for phosphorylated IRE1 α both WT and N906A Fv2E IRE1 *α* showed the presence of phosphorylation of serine 724 IRE1 α in the presence of tetracycline and Ap20187 for 48h. Weak bands of phosphorylated IRE1 α were seen in the presence of just tetracycline for both WT and N906A Fv2E IRE1 α. We therefore have characterised the N906A Fv2E IRE1 α mutant as RNase deficient in chapter 4.3 and Kinase active in chapter 4.4.

4.5 Cell death

We had confirmed that the N906A Fv2E IRE1 α mutant was RNase deficient in chapter 4.3 and that it had retained its kinase activity in chapter 4.4. I decided to test N906A Fv2E IRE1 α mutant for apoptotic activity or cell death. To test the viability of the N906A Fv2E IRE1 α mutant when exposed to tetracycline & AP20187, we used an MTT assay for cell viability as described in (3.3.9) against WT Fv2E IRE1 α previously shown to have reduced viability upon exposure to tetracycline & AP20187 (Nishitoh, 2002, Watson, PhD thesis).

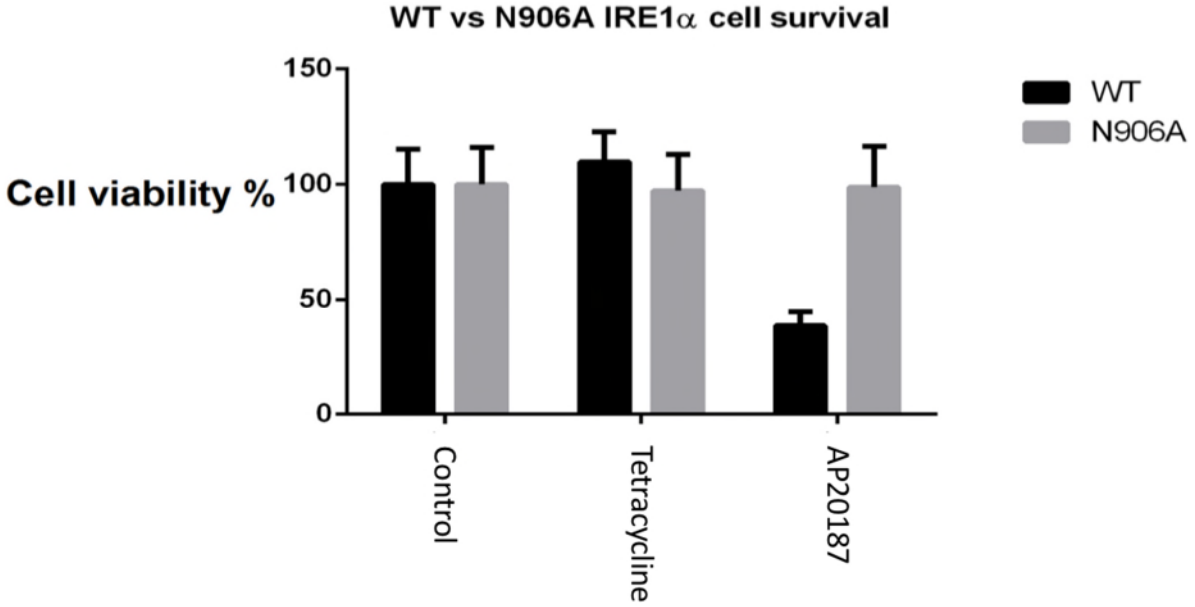

Figure 4.5.1, Flp-In T-Rex HEK293 Fv2E-IRE1 α WT and N906A were treated with tetracycline (1 µg/ml) and AP20187 (200 nM) for 48 h each in a 96 well plate. Three plate repeats were performed, each cell line was cultured in a 96 well plate. Each plate was split so that 8 wells in each plate were used to zero the microplate reader and 22 wells were used for each treatment. Each plate were treated with DMEM medium containing 0.5 mg/ml MTT for 3 h as described in (3.3.9). After treatment, wavelength absorption were taken at 590 nm and 690 nm (reference wavelength) using a microplate reader as detailed in (3.3.9).

Readings were taken at 590 nm as it corresponds to the wavelength on the dissolved dye absorption of electromagnetic radiation formed by oxidation of active cells. We created a comparison of MTT viability results from WT and N906A Fv2E IRE1 α. We tested both cell lines to see if cell viability was affected by treatment of tetracycline (1 µg/ml), as seen in Figure 4.5.1, tetracycline treatment alone did not affect cell viability. We noted that no relevant change in cell viability was detected when N906A Fv2E mutant was exposed to tetracycline and AP20187 for 48h unlike WT Fv2E IRE1 α that had a significant decrease in cell viability. Figure 4.5.1, shows that N906A Fv2E IRE1 α viability is not affected by treatment with tetracycline and AP20187. This proposes that the Kinase activity of IRE1 α signalling alone does not lead to apoptotic signalling.

4.6 WT & N906A Fv2E IRE1 α phosphorylation of JNK

To investigate this model and the reasons behind the viability of the N906A Fv2E IRE1 α exposed to tetracycline and AP20187 we chose to investigate phosphorylation of JNK as a marker for apoptosis (Dhanasekaran and Reddy, 2008). P-JNK is marker known for cell stress

and has been shown to be activated due to IRE1 α signalling, therefore we used it as a marker for apoptotic signalling capability of N906A Fv2E IRE1 α.

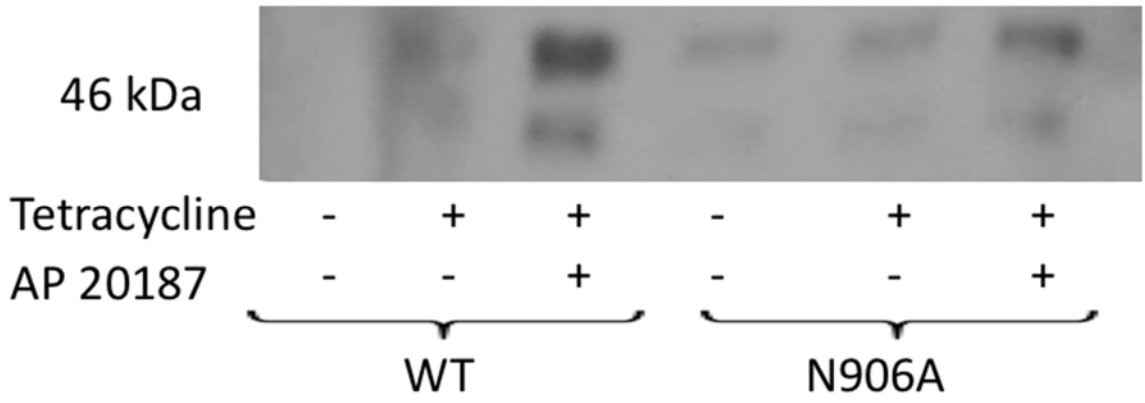

Figure 4.6.1, Flp-In T-Rex HEK293 Fv2E-IRE1 α WT and N906A were treated with tetracycline (1 µg/ml) and AP20187 (200 nM) for 48h. Cell lysate was extracted as described in (3.3.10) for Western blotting. Cell lysate was Western blotted as described in (3.4) with anti-P-JNK.

The Western blot of Phospho-JNK with WT Fv2E IRE1 α and N906A Fv2E IRE1 α mutants showed a strong band with the WT when exposed to tetracycline and AP20187 for 48 h as seen in Figure 4.6.1. The N906A mutant did show some activation of P-JNK activation in the control, tetracycline, tetracycline and AP20187. The downstream signalling of N906A Fv2E-IRE1 α through P-JNK seems to show stronger activation under tetracycline and AP20187, given the results of chapter 4.5 we conclude that this signalling is not sufficient to induce apoptosis.

4.7 PARP-1 Cleavage

To further investigate the results of chapter 4.5 and 4.5 we explored other markers for apoptosis. We chose to investigate poly(ADP-ribose) polymerase (PARP-1). PARP-1 cleavage is a useful hallmark of apoptosis (Chaitanya, Alexander and Babu, 2010), it is cleaved by DEVD-ase caspases activated during apoptosis.

To obtain data on the downstream signalling of Fv2E-IRE1 α, Flp-In T-Rex HEK293 Fv2E-IRE1 α WT and N906A cells were treated with tetracycline (1 µg/ml) or tetracycline (1 µg/ml) AP20187 (200 nM) for 48 h. Protein lysate was extracted as described in (3.3.10) then separated via gel electrophoresis for Western blotting against an anti-PARP-1 antibody as described in (3.4).

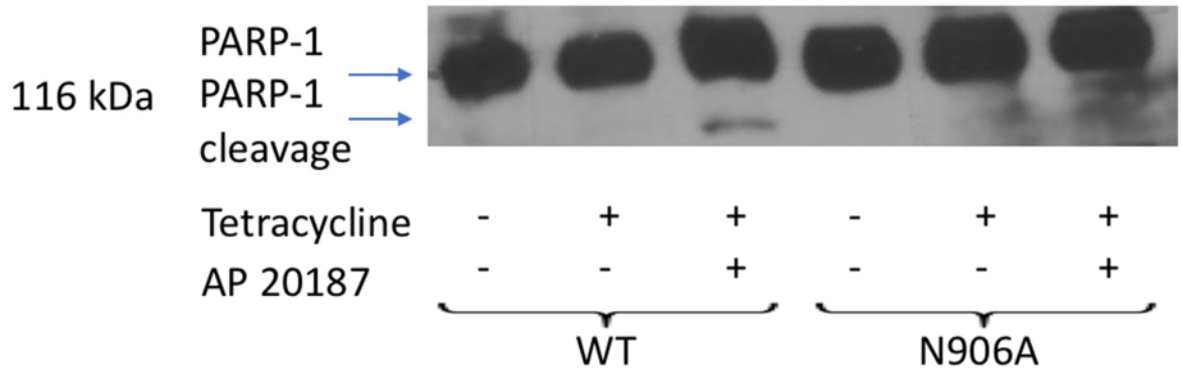

Figure 4.7.1, Flp-In T-Rex HEK293 Fv2E-IRE1 α WT and N906A were treated with tetracycline (1 µg/ml) and AP20187 (200 nM) for 48h. Cell lysate was extracted as described in (2.2.20) for Western blotting. Cell lysate was Western blotted as described in (3.4) with anti-PARP1.

Western blotting results in Figure 4.7.1, showed clear cleavage in WT Fv2E IRE1 α exposed to tetracycline and AP20187 while the N906A mutant had no clear cleavage band although I was unable to produce a clear image. We were unable to clearly characterise the PARP-1 response of N906A; it is possible that cleavage combined with impurities in the gel could explain the unclear results seen for Figure 4.7.1, Fv2E IRE1 α N906A with tetracycline + AP20187 treatment.

To explain these results, I needed to investigate the upstream signalling of PARP-1 and JNK. I decided to investigate IRE1 α kinase domain interaction with TRAF 2.

4.8 Immunoprecipitation of TRAF2

To understand IRE1 α kinase domain we must look at its interaction with the kinase domain-mediated signalling cascade adaptor protein TRAF2 (Urano et al., 2000). As can be seen in Figure 1.7.1, phosphorylated IRE1 α apoptotic pathway is believed to originate with its interaction with TRAF2 leading to activation of ASK1 and phosphorylation of JNK as seen in Chapter 4.4 (Kadowaki and Nishitoh, 2013). This apoptotic pathway leads to the activation of key apoptotic cell death protein markers such as PARP-1 cleavage investigated in Chapter 4.7 (Chaitanya, Alexander and Babu, 2010). To investigate this interaction, we must understand the interaction between N906A Fv2E IRE1 α and TRAF2, to do this we explored isolating TRAF2 with IRE1 α from cell lysate immediately after extraction through immunoprecipitation.

To investigate the lack of apoptotic cell death we tested Fv2E IRE1 α N906A interaction with TRAF2 through immunoprecipitation which has previously been used to detect IRE1 α – TRAF2 interactions. Flp-In T-Rex HEK293 Fv2E-IRE1 α WT and N906A were treated with tetracycline (1 µg/ml) or tetracycline (1 µg/ml) and AP20187 (200 nM) for 48 h with a control with no treatment. Immunoprecipitation was performed as described in chapter 3.4.5. Cell lysate for this immunoprecipitation experiment was extracted from the HEK293 cells as described in Chapter 3.3.10. We determined the concentration of protein before adding 250 µg of protein to 20 µl of protein A-agarose beads for pre-clearing immediately after extraction. The reasoning behind the immediate immunoprecipitation after extraction of the cell lysate is to prevent the interaction of TRAF2 and IRE1 α after extraction from the

cell. We exposed the newly extracted cell lysate to the Protein A-agarose beads, we did this immediately to prevent artificial interactions caused by freeze thaw cycles. I did this initially to remove unspecific integrators, with the beads or protein A. Pre-cleared lysate was incubated with fresh protein A-agarose beads before repeated washing. The washed protein A-agarose beads were then Western blotted as described in Chapter 3.4 with an anti-TRAF2 antibody.

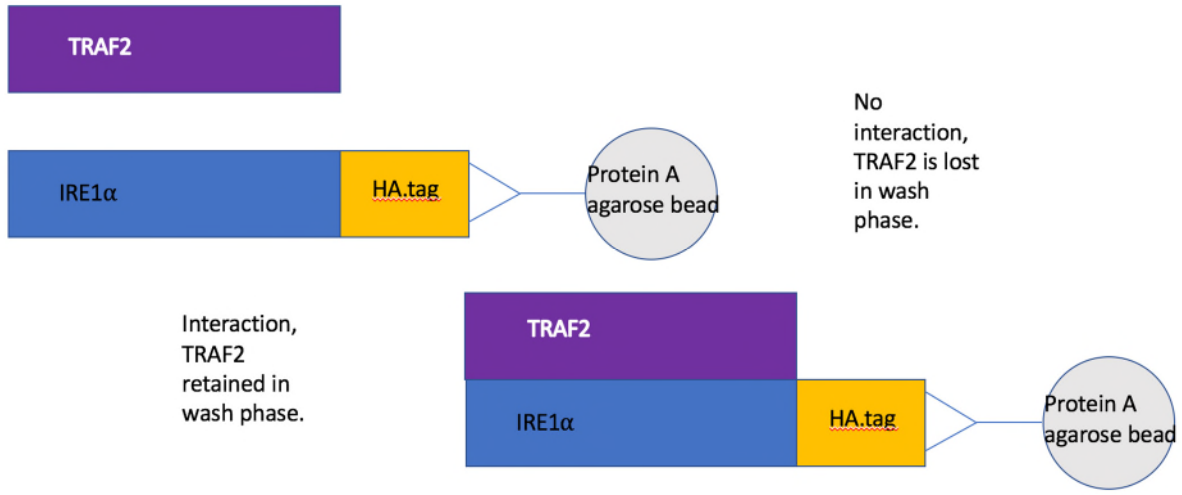

Figure 4.8.2, Immunoprecipitation of TRAF2 using an HA.tag antibody and HA.tag Fv2E IRE1 α. Protein A agarose beads are mixed with anti-HA tag antibodies, the anti-HA antibodies bind to the protein A agarose beads. IRE1 α contains HA.tag sequence that binds to anti-HA antibody Protein A complex. Protein lysate is mixed then subsequently washed after centrifugation, proteins bound to the agarose beads are concentrated in the remaining solution. Active IRE1 α interacts and forms a complex with TRAF2 resulting in TRAF2 presence in lysate through Immunoprecipitation.

We initially used a rabbit anti-TRAF2 primary antibody with an anti-rabbit secondary antibody. Western blotting through this method was unreadable due to background interference. I decided that the HA.tag rabbit primary antibody for immunoprecipitation as shown in Figure 4.8.2, was not denatured in the heating step as described in (3.4) and bound to the secondary antibody during Western blotting. I used a mouse anti-TRAF2 primary antibody in combination with an anti-mouse secondary antibody to solve this issue. Repeated anti-TRAF2 Western blotting of HA.tag immunoprecipitation failed to produce a band for TRAF2 at 55 kDa in the Fv2E WT/N906A IRE1 α exposed to tetracycline and AP20187 for 48h. Explanation of these results is discussed in 5.8.

5. Discussion

5.1 Investigation of Fv2E K907A IRE1 α lack of expression in HEK 293 T-REx cells

The Fv2E K907A, N906A and H910N *IRE1 α* mutants were obtained from another lab. Given that the transfection of *pcDNA5/FRT/TO-Fv2E-IRE1 α* K907A this mutant did not produce a Fv2E IRE1 α K907A in HEK293 cells we decided to investigate this through sequencing. Sequencing of K907A plasmid as described in chapter 2.10 showed that the plasmid contained the ERN1 gene but not the Fv2E domains. This region is responsible for the mutant's cytosolic nature. This mutant protein would be induced by tetracycline would not be cytoplasmic and therefore would not be detected by Western blotting of the cell lysate.

5.2 Assessment of RNase domain activity through XBP1 splicing assays

As the XBP1 splicing assay control demonstrated that the Fv2E IRE1 α chimera retained its RNase activity (Figure 4.3.1). I chose the 48 h AP20187 treatment time period as the control XBP1 splicing assay did not show any un-spliced XBP1.

By using this time point I found that H910N Fv2E IRE1 α mutant retained partial activity of the RNase domain as seen in Figure 4.3.2, Although substitution of a key amino acid did affect the expression this site alone does not seem to completely remove the RNase activity of Fv2E IRE1 α chimera although this was predicted in Han et al., 2009. As the mutant retained activity it is likely that this amino acid plays a large role in IRE1 α RNase activity but further mutations would be required to remove the activity completely. The K907A Fv2E IRE1 α mutant did not show XBP1 splicing in Figure 4.3.2, although this was explained in chapter 5.1 as this mutant did not produce the cytosolic protein and the Fv2E chimera RNase activity is still to be characterised.

The N906A mutant as seen in Figure 4.3.2, did not show the presence of XBP1s in the XBP1 splicing assay. Therefore, the N906A mutation removes the RNase activity beyond detectable levels and was suitable for further testing of in this project. Given that the N906A mutation created a Kinase active and RNase deficient mutant IRE1 α, this area of the protein could be a viable site for creating future RNase deficient mutants. Future experiments could attempt to create mutants with key mutations in this area (836-961 aa) to create a Fv2E IRE1 α mutant to explore this possibility. As will be discussed in chapter 5.8 mutations can interfere with p-IRE1 α interaction with TRAF2 and the Kinase apoptotic pathway, it is possible that this region has a higher probability of producing RNase deficient mutant but could prevent the Kinase domain interaction with TRAF2 therefore these mutants might not confirm whether the kinase domain alone can cause apoptosis.

5.3 Apoptotic cell death

The MTT test establishes cell viability, the test doesn't distinguish the pathway through cell death occurs. Although N906 Fv2E IRE1 α remain viable implies that the kinase signalling pathway has not been activated or that it is not causing apoptosis in this mutant. Therefore, to investigate why apoptosis is not occurring in the N906A Fv2E IRE1 α mutant we must

investigate the mechanisms surrounding IRE1 α Kinase mediated apoptosis. To do this we looked at P-JNK a downstream signaller of TRAF2 (Nishitoh, 2002) and PARP-1 a recognised signal protein (Chaitanya, Alexander and Babu, 2010) for apoptosis to investigate the mechanisms of the N906A Fv2E IRE1 α mutant. An alternative hypothesis to explain these results is that apoptotic signalling of IRE1 α is dependent on the RNase domain. Han et al. 2009 also showed that in kinase active, RNase deficient mutant did not lead to cell death in INS-1 cells with K907A & N906A mutant, chapter 4.5 shows that this fate also occurs in HEK 293 cells for N906A mutants.

5.4 Immunoprecipitation of TRAF2

Given issues with reagents for immunoprecipitation of TRAF2 with IRE1 α, the issue is unlikely to reside with the antibody's as anti-IRE1 α produced results in chapter 4.2 Figure 4.2.1. Issues with TRAF2 Western blotting were overcome through replacement of the primary and secondary antibody as well as changing species for primary antibody, Western blotting of whole cell lysate for TRAF2 confirmed bands therefore there remains two possibilities for the remaining issue, these are explained below.

One possibility for the failure to detect TRAF2 in the extract could be that the TRAF2 or the Fv2E IRE1α TRAF2 complex is removed from the agarose beads through the successive washing steps as described in chapter 3.4.5. The procedure has been successful in other research by our lab, further (Moser, Chan and Fritzler, 2009) optimisation of the procedure could have yielded retention of TRAF2 in the extract and detection in anti-TRAF2 Western blotting. Preparing samples with different numbers of washing steps then Western blotting would find the number of washes that bound TRAF2 is retained while removing non bound TRAF2.

The second possibility is that the issue resides with the agarose beads, given that the reagent is stored at +4˚C (recommended storage conditions 1 year) it was likely to have expired. The affinity of the beads to antibodies since purchase could have reduced resulting in the loss of the TRAF2-pIRE1 α complex through the washing steps resulting in the lack of TRAF2 detected in the Western blotting. It is possibly that replacement of the reagent could have resolved whether Fv2E N906A IRE1 α interacts with TRAF2. Replacement of this reagent with a newer system for immunoprecipitation such as magnetic agarose beads, could have increased the yield of TRAF2 through washing steps.

5.5 IRE1 α phosphorylation

Although we were unable to confirm if N906A Fv2E IRE1 α interacted with TRAF2 to explain the results of 4.6, it is possible that the Fv2E IRE1 α N906A does interact with TRAF2 without leading to apoptosis. Given that P-IRE1 α antibody only indicates phosphorylation of serine 724 IRE1 α, other sites on IRE α might remain un-phosphorylated in the N906A mutant. Although IRE1 α phosphorylation site (serine 724) was phosphorylated, this proteins kinase domain may not have the same characteristics as the wild type due to the level of phosphorylation.

To explore this possibility, we could measure the level of phosphorylation of Fv2E IRE1 α against the WT. To do this we could use radioactive labelled phosphorus through ATP as used in Han et al., 2009. This experiment could be explored to explain the lack of apoptosis in N906A Fv2E IRE1 α seen in 4.5. Given that in Han et al. 2009 kinase active, RNase dead mutants in INS-1 cells did not show apoptosis; a likely explanation from this paper is that kinase active, RNase dead mutants HEK 293 cells do not cause apoptosis. To investigate this theory we should explore immunoprecipitation, this experiment would confirm any interactions between N906A Fv2E IRE1 α and TRAF2. Further investigation of kinase dead, RNase dead mutants interaction with TRAF2 could confirm that mutations in the kinase domain prevent interaction and activation of the TRAF2 pathway. This would explain the Western blotting results seen in chapter 4.4 and Figure 4.4.1, for kinase activity, although the mutant would bind to anti-p-IRE1 α through Western blotting as antibody only binds to one phosphorylation site. If only this phosphorylation site is active other phosphorylation sites required for kinase activity with TRAF2 might remain un-phosphorylated, preventing the apoptotic signalling and resulting in the lack of apoptosis seen in chapter 4.5.

5.6 Conclusion

If a kinase active RNase IRE1 α mutant retained its apoptotic function, given the loss of the protective actions of the RNase domain the percentage of cell death should be higher than that seen in the WT Fv2E IRE1 α Figure 4.5.1. Although we were unable to measure the interaction between N906A IRE1α and TRAF2; given that we have seen activation of p-JNK and possible cleavage of PARP-1 the affinity of the IRE1 α-TRAF2 interaction might be sufficient to cause apoptotic signalling without sufficient intensity to cause apoptosis. Additionally, as discussed in chapter 5.5 partial phosphorylation of IRE1 α could lead to the results seen. If the level of phosphorylation affects the activation and signalling of apoptosis via TRAF2. The level of activation of a partially phosphorylated IRE1 α could show some p-JNK activation but no PARP-1 cleavage therefore showing no noticeable cell death explaining the results of Figure 4.5.1, MTT test for cell viability. Given the results in Han et al. 2009 with INS-1 cells apoptosis caused by IRE1 α pathway could require interaction from an active IRE1 α RNase domain to cause apoptosis. Although this research was inconclusive creation of further kinase active RNase dead mutants might reveal the true characterisation of the IRE1 α kinase and RNase domain roles in eukaryotic cells.

6. Bibliography

Aragón, T., van Anken, E., Pincus, D., Serafimova, I., Korennykh, A., Rubio, C. and Walter, P. (2008). Messenger RNA targeting to endoplasmic reticulum stress signalling sites. *Nature*, 457(7230), pp.736-740.

Calfon, M., Zeng, H., Urano, F., Till, J., Hubbard, S., Harding, H., Clark, S. and Ron, D. (2002). corrigendum: IRE1 couples endoplasmic reticulum load to secretory capacity by processing the XBP-1 mRNA. *Nature*, 420(6912), pp.202-202.

Chaitanya, G., Alexander, J. and Babu, P. (2010). PARP-1 cleavage fragments: Signatures of cell-death proteases in neurodegeneration. *Cell Communication and Signaling*, 8(1), p.31.

Dhanasekaran, D. and Reddy, E. (2008). JNK signaling in apoptosis. *Oncogene*, 27(48), pp.6245-6251.

Cox, J. and Walter, P. (1996). A novel mechanism for regulating activity of a transcription factor that controls the unfolded protein response. *Cell*, 87(3), pp.391-404.

Cox, J., Shamu, C. and Walter, P. (1993). Transcriptional induction of genes encoding endoplasmic reticulum resident proteins requires a transmembrane protein kinase. *Cell*, 73(6), pp.1197-1206.

Credle, J., Finer-Moore, J., Papa, F., Stroud, R. and Walter, P. (2005). On the mechanism of sensing unfolded protein in the endoplasmic reticulum. *Proceedings of the National Academy of Sciences*, 102(52), pp.18773-18784.

Dong, M., Bridges, J., Apsley, K., Xu, Y. and Weaver, T. (2008). ERdj4 and ERdj5 are required for endoplasmic reticulum-associated protein degradation of misfolded surfactant protein C. *Molecular Biology of the Cell*, 19(6), pp.2620-2630.

Gonzalez, T. (1999). Mechanism of non-spliceosomal mRNA splicing in the unfolded protein response pathway. *The EMBO Journal*, 18(11), pp.3119-3132.

Han, D., Lerner, A., Vande Walle, L., Upton, J., Xu, W., Hagen, A., Backes, B., Oakes, S. and Papa, F. (2009). IRE1α kinase activation modes control alternate endoribonuclease outputs to determine divergent cell fates. *Cell*, 138(3), pp.562-575.

Harding, H., Zeng, H., Zhang, Y., Jungries, R., Chung, P., Plesken, H., Sabatini, D. and Ron, D. (2001). Diabetes mellitus and exocrine pancreatic dysfunction in perk−/− mice reveals a role for translational control in secretory cell survival. *Molecular Cell*, 7(6), pp.1153-1163.

Ichijo, H. (1997). Induction of apoptosis by ASK1, a mammalian MAPKKK that activates SAPK/JNK and p38 signaling pathways. *Science*, 275(5296), pp.90-94.

Imai, Y., Soda, M., Inoue, H., Hattori, N., Mizuno, Y. and Takahashi, R. (2001). An unfolded putative transmembrane polypeptide, which can lead to endoplasmic reticulum stress, is a substrate of parkin. *Cell*, 105(7), pp.891-902.

Julier, C., Delépine, M., Nicolino, M., Barrett, T., Golamaully, M. and Mark Lathrop, G. (2000). EIF2AK3, encoding translation initiation factor 2-alpha kinase 3, is mutated in patients with wolcott-rallison syndrome. *Nature Genetics*, 25(4), pp.406-409.

Kadowaki, H. and Nishitoh, H. (2013). Signaling pathways from the endoplasmic reticulum and their roles in disease. *Genes*, 4(3), pp.306-333.

Kakizuka, A. (1998). Protein precipitation: a common etiology in neurodegenerative disorders?. *Trends in Genetics*, 14(10), pp.396-402.

Katayama, T., Imaizumi, K., Sato, N., Miyoshi, K., Kudo, T., Hitomi, J., Morihara, T., Yoneda, T., Gomi, F., Mori, Y., Nakano, Y., Takeda, J., Tsuda, T., Itoyama, Y., Murayama, O., Takashima, A., St George-Hyslop, P., Takeda, M. and Tohyama, M. (1999). Presenilin-1 mutations downregulate the signalling pathway of the unfolded-protein response. *Nature Cell Biology*, 1(8), pp.479-485.

Kaufman, R. (2002). Orchestrating the unfolded protein response in health and disease. *Journal of Clinical Investigation*, 110(10), pp.1389-1398.

Korennykh, A., Korostelev, A., Egea, P., Finer-Moore, J., Stroud, R., Zhang, C., Shokat, K. and Walter, P. (2011). Structural and functional basis for RNA cleavage by Ire1. *BMC Biology*, 9(1), p.47.

Kosmaczewski, S., Edwards, T., Han, S., Eckwahl, M., Meyer, B., Peach, S., Hesselberth, J., Wolin, S. and Hammarlund, M. (2014). The RtcB RNA ligase is an essential component of the metazoan unfolded protein response. EMBO reports, 15(12), pp.1278-1285.

Lee, H. and Lee, S. (2002). Characterization of cytoplasmic α-synuclein aggregates. *Journal of Biological Chemistry*, 277(50), pp.48976-48983.

Lee, K., Dey, M., Neculai, D., Cao, C., Dever, T. and Sicheri, F. (2008). Structure of the Dual Enzyme Ire1 Reveals the Basis for catalysis and regulation in nonconventional RNA splicing. *Cell*, 132(1), pp.89-100.

Merksamer, P., Trusina, A. and Papa, F. (2008). Real-time redox measurements during endoplasmic reticulum stress reveal interlinked protein folding functions. *Cell*, 135(5), pp.933-947.

Moser, J., Chan, E. and Fritzler, M. (2009). Optimization of immunoprecipitation–Western blot analysis in detecting GW182-associated components of GW/P bodies. *Nature Protocols*, 4(5), pp.674-685.

Nakagawa, T., Zhu, H., Morishima, N., Li, E., Xu, J., Yankner, B. and Yuan, J. (2000). Caspase-12 mediates endoplasmic-reticulum-specific apoptosis and cytotoxicity by amyloid-β. *Nature*, 403(6765), pp.98-103.

Nishitoh, H. (2002). ASK1 is essential for endoplasmic reticulum stress-induced neuronal cell death triggered by expanded polyglutamine repeats. *Genes & Development*, 16(11), pp.1345-1355.

Nishitoh, H., Saitoh, M., Mochida, Y., Takeda, K., Nakano, H., Rothe, M., Miyazono, K. and Ichijo, H. (1998). ASK1 is essential for JNK/SAPK activation by TRAF2. *Molecular Cell*, 2(3), pp.389-395.

Paulson, H., Bonini, N. and Roth, K. (2000). Polyglutamine disease and neuronal cell death. *Proceedings of the National Academy of Sciences*, 97(24), pp.12957-12958.

Ozcan, L. and Tabas, I. (2012). Role of endoplasmic reticulum stress in metabolic disease and other disorders. *Annual Review of Medicine*, 63(1), pp.317-328.

Ron, D. and Walter, P. (2007). Signal integration in the endoplasmic reticulum unfolded protein response. *Nature Reviews Molecular Cell Biology*, 8(7), pp.519-529.

Saitoh, M. (1998). Mammalian thioredoxin is a direct inhibitor of apoptosis signal-regulating kinase (ASK) 1. *The EMBO Journal*, 17(9), pp.2596-2606.

Shen, X., Ellis, R., Lee, K., Liu, C., Yang, K., Solomon, A., Yoshida, H., Morimoto, R., Kurnit, D., Mori, K. and Kaufman, R. (2001). Complementary signaling pathways regulate the unfolded protein response and are required for *C. elegans* development. *Cell*, 107(7), pp.893-903.

Sidrauski, C., Cox, J. and Walter, P. (1996). tRNA Ligase is required for regulated mRNA splicing in the unfolded protein response. *Cell*, 87(3), pp.405-413.

Tabas, I. and Ron, D. (2011). Integrating the mechanisms of apoptosis induced by endoplasmic reticulum stress. *Nature Cell Biology*, 13(3), pp.184-190.

Thermofisher.com. (2018). *Flp-In System: For Generating Constitutive Expression Cell Lines | Thermo Fisher Scientific*. [online] Available at: https://www.thermofisher.com/uk/en/home/references/protocols/proteins-expression-isolation-and-analysis/protein-expression-protocol/flp-in-system-for-generating-constitutive-expression-cell-lines.html [Accessed 13 Mar. 2018].

Thermofisher.com. (2018). *Inducible Protein Expression Using the T-REx™ System | Thermo Fisher Scientific*. [online] Available at: https://www.thermofisher.com/uk/en/home/references/protocols/proteins-expression-isolation-and-analysis/protein-expression-protocol/inducible-protein-expression-using-the-trex-system.html [Accessed 13 Mar. 2018].

Tirasophon, W. (2000). The endoribonuclease activity of mammalian IRE1 autoregulates its mRNA and is required for the unfolded protein response. *Genes & Development*, 14(21), pp.2725-2736.

Tobiume, K., Matsuzawa, A., Takahashi, T., Nishitoh, H., Morita, K., Takeda, K., Minowa, O., Miyazono, K., Noda, T. and Ichijo, H. (2001). ASK1 is required for sustained activations of JNK/p38 MAP kinases and apoptosis. *EMBO reports*, 2(3), pp.222-228.

Travers, K., Patil, C., Wodicka, L., Lockhart, D., Weissman, J. and Walter, P. (2000). Functional and genomic analyses reveal an essential coordination between the unfolded protein response and ER-associated degradation. *Cell*, 101(3), pp.249-258.

Tsuru, A., Imai, Y., Saito, M. and Kohno, K. (2018). *Novel mechanism of enhancing IRE1α-XBP1 signalling via the PERK-ATF4 pathway*.

Urano, F. (2000). Coupling of stress in the ER to activation of JNK protein kinases by transmembrane protein kinase IRE1. *Science*, 287(5453), pp.664-666.

Watson, Jamie,Nicholas (2017) Characterisation of the contribution of the kinase and RNase activities of Ire1α to activation of apoptotic JNK signalling, Durham theses, Durham University. Available at Durham E-Theses Online: http://etheses.dur.ac.uk/12248/

Welihinda, A., Tirasophon, W., Green, S. and Kaufman, R. (1998). Protein Serine/Threonine phosphatase Ptc2p negatively regulates the unfolded-protein response by dephosphorylating Ire1p kinase. *Molecular and Cellular Biology*, 18(4), pp.1967-1977.

Yoshida, H., Matsui, T., Yamamoto, A., Okada, T. and Mori, K. (2001). XBP1 mRNA is induced by ATF6 and spliced by IRE1 in response to ER Stress to produce a highly active transcription factor. *Cell*, 107(7), pp.881-891.

Zhou, Y., Wang, R., Li, L., Xia, X. and Sun, Z. (2006). Inferring functional linkages between proteins from evolutionary scenarios. *Journal of Molecular Biology*, 359(4), pp.1150-1159.

Yuasa, T., Ohno, S., Kehrl, J. and Kyriakis, J. (1998). Tumor necrosis factor signaling to stress-activated protein kinase (SAPK)/Jun NH2-terminal kinase (JNK) and p38. *Journal of Biological Chemistry*, 273(35), pp.22681-22692.

7. Appendix

7.1 Solutions for protein work

Table 7.1 Solutions for protein work

Solutions	**Protocol**
Electrotransfer buffer	4.20 g NaHCO3 1.59 g Na2CO3 Add 5 l H2O
RIPA Buffer	0.5 ml 1 M Tris·HCl pH 8.0 0.3 ml 5 M NaCl 0.1 ml Triton X-100 0.5 ml 10% (w/v) sodium deoxycholate 0.1 ml 10% (w/v) sodium dodecyl sulphate (SDS) Add H2O to 10 ml Add protease/phosphatase inhibitor as required.
10x Semi-Dry Transfer Buffer	73.19 g Glycine 60.6 g Tris-Base Dissolve in ~350 ml H2O Add DI H2O to 500 ml
1x Semi-Dry Transfer Buffer	50 ml 10 x semi-Dry transfer buffer 25 ml Methanol Add DI H2O to 500 ml
TBST	24.2 g Tris base 80g NaCl 1 ml Tween 20 Dissolve in ~800 ml pH ~ 7.6 Add H2O to 1 l
6 x SDS-PAGE sample buffer	3.50 ml 1 M Tris·HCl 3.78 g glycerol 1.00 g SDS 500 µl 10 g/l bromophenol blue 200 µl β-mercaptoethanol Add H2O to 10 ml
10 x SDS-PAGE running buffer	144.13 g glycine 30.03 g Tris 10.00 g SDS Add H2O to ~ 900 ml, stir until completely dissolved, then add H2O to 1 l.
Stripping solution	1g SDS 350 µl β-mercaptoethanol Dissolve in ~40 ml H2O Add H2O to 50 ml
TBST + 5% (w/v) skimmed milk powder	5 g milk powder Dissolve in 100 ml TBST
TBST + 5% (w/v) BSA 0.5 mg/ml MTT (3-[4,5-Dimethylthiazol-2-yl]-2,5-diphenyltetrazolium bromide; Thiazolyl blue)	0.5 g BSA Dissolve in 10 ml TBST Per 1 ml H_2O: 0.5 mg MTT
Protein A-Agarose Beads	Purchased from Santa Cruz Biotechnology (#sc-2001)

7.2 Solutions for DNA work

Table 7.2 Solutions for DNA work

Solution	Protocol
2 mM dNTPs	910 µl H2O 10 µl 100 mM Tris·HCl (pH 8.0) 20 µl 100 mM dATP 20 µl 100 mM dCTP 20 µl 100 mM dGTP 20 µl 100 mM dTTP
50x TAE	242 g Tris 57.1 ml HOAc 37.2 g Na2EDTA·2H2O Dissolve in ~800 ml H2O Add H2O to 1 l pH ~ 8.5
10x TE (pH 8.0)	400 ml 1 M Tris·HCl (pH 8.0) 80 ml 0.5 M EDTA Add H2O to 4 l Autoclave

7.3 Solutions for RNA work

Table 7.3 Solutions used for RNA work

Solution	Protocol
DEPC-H2O	1 mL DEPC 1 l sterile H2O Autoclave.
2 mM dNTPs	910 µl DEPC treated water 10 µl 100 mM Tris·HCl (pH 8.0) in DEPC treated water. 20 µl 100 mM dATP 20 µl 100 mM dCTP 20 µl 100 mM dGTP 20 µl 100 mM dTTP

7.4 Plasmids Table

Table 7.4 List of plasmids used

Name	Source
pcDNA5/FRT/TO-Fv2E-K907A- C'IRE1 α	Dr. David Cox & Dr. Martin Schröder, Durham University
pcDNA5/FRT/TO-Fv2E-N906A- C'IRE1 α	Dr. David Cox & Dr. Martin Schröder, Durham University
pcDNA5/FRT/TO-Fv2E-H910A- C'IRE1 α	Dr. David Cox & Dr. Martin Schröder, Durham University

7.5 Solutions for bacterial work

Table 7.5 Solutions used for bacterial work

Solution	Protocol
SOC Broth (per Liter)	20 g tryptone 5 g Yeast extract 0.5 g NaCl 2.5 ml 1 M KCl Adjust pH to 7 with 10 M NaOH Make up to 990 ml with dH2O AUTOCLAVE After autoclaving add: 10 ml filter sterilised 1 M MgCl2 20 ml filter sterilised 1 M glucose
2 mM dNTPs	910 µl H2O 10 µl 100 mM Tris·HCl (pH 8.0) 20 µl 100 mM dATP 20 µl 100 mM dCTP 20 µl 100 mM dGTP 20 µl 100 mM dTTP
50x TAE	242 g Tris 57.1 ml HOAc 37.2 g Na2EDTA·2H2O Dissolve in ~800 ml H2O Add H2O to 1 l pH ~ 8.5
10x TE (pH 8.0)	400 ml 1 M Tris·HCl (pH 8.0) 80 ml 0.5 M EDTA Add H2O to 4 l Autoclave